

Full-Duplex Cell-Free mMIMO Systems: Analysis and Decentralized Optimization

Soumyadeep Datta, Ekant Sharma, D.N. Amudala, Rohit Budhiraja and Shivendra S. Panwar, *Fellow*, IEEE

Abstract

Cell-free (CF) massive multiple-input-multiple-output (mMIMO) deployments are usually investigated with half-duplex nodes and high-capacity fronthaul links. To leverage the possible gains in throughput and energy efficiency (EE) of full-duplex (FD) communications, we consider a FD CF mMIMO system with *practical limited-capacity fronthaul links*. We derive closed-form spectral efficiency (SE) lower bounds for this system with maximum-ratio combining/maximum-ratio transmission processing and optimal uniform quantization. We then optimize the weighted sum EE (WSEE) via downlink and uplink power control by using a two-layered approach: the first layer formulates the optimization as a generalized convex program, while the second layer solves the optimization decentrally using alternating direction method of multipliers. We analytically show that the proposed two-layered formulation yields a Karush-Kuhn-Tucker point of the original WSEE optimization. We numerically show the influence of weights on the individual EE of the users, which demonstrates the utility of WSEE metric to incorporate heterogeneous EE requirements of users. We show that the low fronthaul capacity reduces the number of users each AP can support, and the cell-free system, consequently, becomes user-centric.

Index Terms

Decentralized optimization, energy efficiency, full-duplex (FD), limited-capacity fronthaul.

I. INTRODUCTION

Massive multiple-input-multiple-output (mMIMO) wireless systems employ a large number of antennas at the base-stations (BSs), and achieve higher spectral efficiency (SE) and energy efficiency (EE) with relatively simple signal processing [1]–[3]. Two distinct mMIMO variants are being investigated in the literature: i) co-located, wherein all antennas are located at one place [1]; and ii) distributed, wherein antennas are spread over a large area [2], [3]. While co-located mMIMO systems have a low fronthaul requirement, distributed mMIMO systems, at the cost of higher fronthaul infrastructure, have greater spatial diversity to exploit and consequently have greater immunity to shadow fading [2]. Cell-free (CF) mMIMO is one of the most

Soumyadeep Datta, Dheeraj Naidu Amudala and Rohit Budhiraja are with IIT Kanpur 208016, India. email: {sdatta, dheeraja, rohitbr}@iitk.ac.in. Ekant Sharma is with IIT Roorkee 247667, India. email: ekant@ece.iitr.ac.in. Soumyadeep Datta and Shivendra S. Panwar are with NYU Tandon School of Engineering, Brooklyn, NY 11201, USA. email: {sd3927, sp1832}@nyu.edu. A part of this work is accepted in IEEE ICC 2021.

promising distributed mMIMO variants in the current literature [2], [3]. CF mMIMO envisions a communication region with no cell boundaries, and promises substantial gains in SE and fairness over small-cell deployments [2], [3].

Full-duplex (FD) wireless systems have now been practically realized with advanced self-interference (SI) cancellation mechanisms [4]. FD CF mMIMO is a relatively recent area of interest [5]–[7], where access points (APs) simultaneously serve downlink and uplink user equipments (UEs) on the same spectral resource. Vu *et al.* in [5] considered a FD CF mMIMO system with maximum-ratio combining and showed that if SI at the APs is suppressed up to a certain limit, it has higher throughput than its half-duplex (HD) counterpart and FD co-located systems. Wang *et al.* in [6] evaluated the SE of a network-assisted FD CF mMIMO system using zero-forcing and regularized zero-forcing beamforming. Reference [7] proposed a heap-based algorithm for pilot assignment to overcome pilot contamination in FD CF mMIMO systems.

In CF mMIMO, APs are connected to a central processing unit (CPU) using fronthaul links. The existing FD CF mMIMO literature assumes high-capacity fronthaul links [5]–[7]. These links, however, have limited capacity, and the information needs to be consequently quantized and sent over them. The limited-capacity fronthaul has been considered only for HD CF mMIMO systems in [8]–[10]. Femenias *et al.* in [9] formulated a max-min uplink/downlink power allocation problem for HD CF mMIMO with limited-capacity fronthaul, while Masoumi *et al.* in [10] optimized the SE of a HD CF mMIMO uplink with limited-capacity fronthaul and hardware impairments. Bashar *et al.* in [8] derived the SE of HD CF mMIMO uplink with limited-capacity fronthaul. We consider quantized- fronthaul for a FD CF mMIMO system to derive achievable SE expressions. To the best of our knowledge, the current work is first one to do so.

With tremendous increase in network traffic, the EE has become an important metric to design a modern wireless system. Global energy efficiency (GEE), defined as the ratio of the network SE and its total energy consumption, is being used to design CF mMIMO communication systems [11]–[14]. Ngo *et al.* in [11] optimized the GEE for the downlink of HD CF mMIMO system. Bashar *et al.* in [12] optimized the uplink GEE of a HD CF mMIMO system with optimal uniform fronthaul quantization. Alonzo *et al.* in [13] optimized the GEE of CF and UE-centric HD mMIMO deployments in the mmWave regime. Nguyen *et al.* in [14] maximized a novel SE-GEE metric for the FD CF mMIMO system using a Dinkelbach-like algorithm.

A UE with limited energy availability will accord a much higher importance to its EE than

an another UE with a sufficient energy supply. GEE is a network-centric metric and cannot accommodate such heterogeneous EE requirements [15]. The weighted sum energy efficiency (WSEE) metric, defined as the weighted sum of individual EEs [15], can prioritize EEs of individual UEs, by allocating them a higher weight [16], [17]. The WSEE metric is investigated in [16] and for a general wireless network in [17] for a two-way FD relay. It is yet to be investigated for CF mMIMO HD and FD systems.

Decentralized designs, which accomplish a complex task by coordination and cooperation of a set of computing units, are being used to design mMIMO systems [18], [19]. This interest is driven by high computational complexity and high interconnection data rate requirements between radio-frequency chains and baseband units in centralized mMIMO system designs [18]. Jeon *et al.* in [18] constructed decentralized equalizers by partitioning the BS antenna array. Reference [19] proposed a coordinate-descent-based decentralized algorithm for mMIMO uplink detection and downlink precoding. Reference [20] employed alternating direction method of multipliers (ADMM) to decentrally allocate edge-computing resource for vehicular networks. Reference [21] applied ADMM to decentrally maximize the WSEE for a two-way HD relay. Such decentralized approaches have not yet been employed to optimize FD CF mMIMO systems. We next list our **main** contributions in this context:

- 1) We consider FD CF mMIMO communications with maximal ratio combining/maximal ratio transmission (MRC)/(MRT) processing and limited fronthaul with optimal uniform quantization. This is unlike the existing works on FD CF mMIMO [5]–[7], [14], which consider perfect high-capacity fronthaul links. We derive achievable SE expressions for both uplink and downlink UEs, which are valid for arbitrary number of antennas at each AP. We use the derived SE expression to maximize the non-convex WSEE metric. While energy-efficient design of CF mMIMO systems have been studied in literature [11]–[14], most of them focus on the GEE metric, except reference [14]. The GEE, being a single ratio, can be expressed as a pseudo-concave (PC) function and can thus be maximized using Dinkelbach’s algorithm [15]. Reference [14] is the only work so far which optimized the EE of FD CF mMIMO. It considered a novel SE-GEE objective, which also reduces to a PC function and is maximized using a Dinkelbach-like algorithm. *The WSEE, in contrast, is a sum of PC functions, and is not guaranteed to be a PC function [15]. This makes the WSEE an extremely non-trivial objective to maximize [15].* Further, the algorithm in [14] requires knowledge of instantaneous small-scale channel

fading coefficients. The WSEE metric optimized here, in contrast, requires large-scale channel coefficients, which remains constant for multiple coherence intervals [2].

2) We decentrally maximize WSEE using a two-layered iterative approach combining successive convex approximation (SCA) and ADMM. The first layer simplifies the non-convex WSEE maximization problem, by using epigraph transformation, slack variables and series approximations. It then locally approximates the problem as a generalized convex program (GCP) which is solved iteratively using the SCA approach. The second layer decentrally optimizes the GCP by using the consensus ADMM approach, which decomposes the centralized version into multiple sub-problems, each of which is solved independently. The local solutions are combined to obtain the global solution. We note that the GCP is not in the standard form which is required for applying ADMM, as it involves constraints that couple power control coefficients from different UEs. We therefore create global and local versions of the power control coefficients, which decouple the constraints, and iteratively update them till the algorithm converges.

3) We show that there is a fundamental limit to the number of UEs a FD AP can serve with limited fronthaul capacity by imposing impose separate constraints on the number of uplink and downlink UEs. We propose a *proportionately-fair* rule capping the maximum number of uplink and downlink UEs served by each AP. We use this rule to propose a fair AP selection algorithm which efficiently chooses the best subset of APs to serve each uplink and downlink UE.

4) We analytically and numerically prove the convergence of the proposed decentralized approach. We numerically demonstrate the tightness of our obtained achievable SE expressions and investigate its variation with various system model parameters. We numerically show that the proposed decentralized optimization i) achieves the same WSEE as the centralized approach; and ii) is responsive to changing weights which can be set to prioritize UEs' EE requirements.

II. SYSTEM MODEL

We consider, as shown in Fig. 1, a FD CF mMIMO system where M FD APs serve K single-antenna HD UEs on the same spectral resource, comprising K_u UEs on the uplink and K_d UEs on the downlink, with $K = (K_u + K_d)$. Each AP has N_t transmit antennas and N_r receive antennas, and is connected to the CPU using a limited-capacity fronthaul link which carries quantized uplink/downlink information to/from the CPU. From Fig. 1, due to FD model,

- uplink receive signal of each AP is interfered by its own downlink transmit signal (intra-AP) and that of other APs (inter-AP) (shown as purple (resp. brown) lines on (resp. between) APs).

- downlink UEs receive transmit signals from uplink UEs, causing uplink downlink interference (UDI) (shown as black dotted lines between uplink and downlink UEs). Additionally, the UEs experience multi-UE interference (MUI) as the APs serve them on the same spectral resource.

We next explain various channels, their estimation and data transmission. We assume a coherence interval of duration T_c (in s) with τ_c samples, which is divided into: a) channel estimation phase of τ_t samples, and b) downlink and uplink data transmission of $(\tau_c - \tau_t)$ samples.

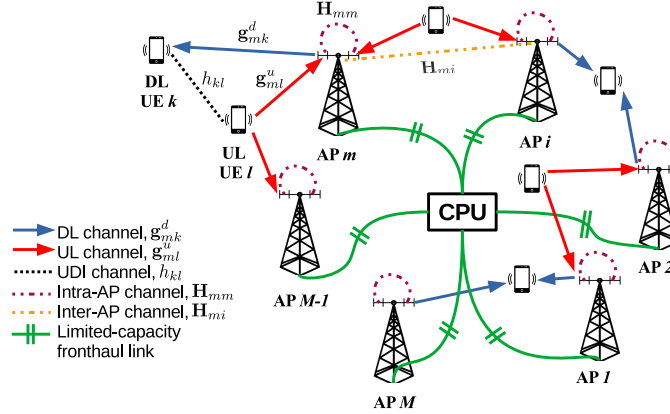


Fig. 1: System model for FD CF mMIMO communications

Channel description: The channel of the k th downlink UE to the transmit antennas of the m th AP is $\mathbf{g}_{mk}^d \in \mathbb{C}^{N_t \times 1}$, while the channel from the l th uplink UE to the receive antennas of the m th AP is $\mathbf{g}_{ml}^u \in \mathbb{C}^{N_r \times 1}$.¹ We model these channels as $\mathbf{g}_{mk}^d = (\beta_{mk}^d)^{1/2} \tilde{\mathbf{g}}_{mk}^d$ and $\mathbf{g}_{ml}^u = (\beta_{ml}^u)^{1/2} \tilde{\mathbf{g}}_{ml}^u$. Here β_{mk}^d and $\beta_{ml}^u \in \mathbb{R}$ are corresponding large scale fading coefficients, which are same for all antennas at the m th AP [2], [5]. The vectors $\tilde{\mathbf{g}}_{mk}^d$ and $\tilde{\mathbf{g}}_{ml}^u$ denote small scale fading with independent and identically distributed (i.i.d.) $\mathcal{CN}(0, 1)$ entries. The UDI channel between the k th downlink UE and l th uplink UE is modeled as $h_{kl} = (\tilde{\beta}_{kl})^{1/2} \tilde{h}_{kl}$ [5], [6], where $\tilde{\beta}_{kl}$ is the large scale fading coefficient and $\tilde{h}_{kl} \sim \mathcal{CN}(0, 1)$ is the small scale fading. The inter- and intra-AP channels from the transmit antennas of the i th AP to the receive antennas of the m th AP are denoted as $\mathbf{H}_{mi} \in \mathbb{C}^{N_r \times N_t}$, $i = 1$ to M .

Uplink channel estimation: Recall that the channel estimation phase consists of τ_t samples. We divide them as $\tau_t = \tau_t^d + \tau_t^u$, where τ_t^d and τ_t^u are samples used as pilots for the downlink and uplink UEs, respectively. All the downlink (resp. uplink) UEs simultaneously transmit τ_t^d (resp. τ_t^u)-length uplink pilots to the APs, which they use to estimate the respective channels. In this phase, both transmit and receive antenna arrays of each AP, similar to [5], operate in receive

¹We, henceforth, consider $k = 1$ to K_d , $l = 1$ to K_u and $m = 1$ to M , to avoid repetition, unless mentioned otherwise.

mode. The k th downlink UE (resp. l th uplink UE) transmits pilot signals $\sqrt{\tau_t^d} \boldsymbol{\varphi}_k^d \in \mathbb{C}^{\tau_t^d \times 1}$ (resp. $\sqrt{\tau_t^u} \boldsymbol{\varphi}_l^u \in \mathbb{C}^{\tau_t^u \times 1}$). We assume, similar to [5], [11], that the pilots i) have unit norm i.e., $\|\boldsymbol{\varphi}_l^u\| = \|\boldsymbol{\varphi}_k^d\| = 1$; and ii) are intra-set orthonormal i.e. $(\boldsymbol{\varphi}_l^u)^H \boldsymbol{\varphi}_{l'}^u = 0 \forall l \neq l'$ and $(\boldsymbol{\varphi}_k^d)^H \boldsymbol{\varphi}_{k'}^d = 0 \forall k \neq k'$. Therefore, we need $\tau_t^d \geq K_d$ and $\tau_t^u \geq K_u$ [5], [11].

The pilots received by transmit and receive antennas of the m th AP are given respectively as

$$\mathbf{Y}_m^{tx} = \sqrt{\tau_t^d \rho_t} \sum_{k=1}^{K_d} \mathbf{g}_{mk}^d (\boldsymbol{\varphi}_k^d)^H + \mathbf{W}_m^{tx}, \text{ and } \mathbf{Y}_m^{rx} = \sqrt{\tau_t^u \rho_t} \sum_{l=1}^{K_u} \mathbf{g}_{ml}^u (\boldsymbol{\varphi}_l^u)^H + \mathbf{W}_m^{rx}.$$

Here ρ_t is the normalized pilot transmit signal-to-noise-ratio (SNR). The matrices $\mathbf{W}_m^{tx} \in \mathbb{C}^{N_t \times \tau_t^d}$ and $\mathbf{W}_m^{rx} \in \mathbb{C}^{N_r \times \tau_t^u}$ denote additive noise with $\mathcal{CN}(0, 1)$ entries. Each AP independently estimates its channels with the uplink and downlink UEs to avoid channel state information (CSI) exchange overhead [5], [14]. To estimate the channels \mathbf{g}_{mk}^d and \mathbf{g}_{ml}^u , the m th AP projects the received signal onto the pilot signals $\boldsymbol{\varphi}_k^d$ and $\boldsymbol{\varphi}_l^u$ respectively, as $\hat{\mathbf{g}}_{mk}^{tx} = \mathbf{Y}_m^{tx} \boldsymbol{\varphi}_k^d = \sqrt{\tau_t^d \rho_t} \mathbf{g}_{mk}^d + \mathbf{W}_m^{tx} \boldsymbol{\varphi}_k^d$ and $\hat{\mathbf{g}}_{ml}^{rx} = \mathbf{Y}_m^{rx} \boldsymbol{\varphi}_l^u = \sqrt{\tau_t^u \rho_t} \mathbf{g}_{ml}^u + \mathbf{W}_m^{rx} \boldsymbol{\varphi}_l^u$. These projections are used to compute the corresponding linear minimum-mean-squared-error (MMSE) channel estimates [5] as $\hat{\mathbf{g}}_{mk}^d = \mathbb{E}\{\mathbf{g}_{mk}^d (\hat{\mathbf{g}}_{mk}^{tx})^H\} (\mathbb{E}\{\hat{\mathbf{g}}_{mk}^{tx} (\hat{\mathbf{g}}_{mk}^{tx})^H\})^{-1} \hat{\mathbf{g}}_{mk}^{tx}$, $\hat{\mathbf{g}}_{ml}^u = \mathbb{E}\{\mathbf{g}_{ml}^u (\hat{\mathbf{g}}_{ml}^{rx})^H\} (\mathbb{E}\{\hat{\mathbf{g}}_{ml}^{rx} (\hat{\mathbf{g}}_{ml}^{rx})^H\})^{-1} \hat{\mathbf{g}}_{ml}^{rx} = c_{ml}^u \hat{\mathbf{g}}_{ml}^{rx}$, where $c_{mk}^d = \frac{\sqrt{\tau_t^d \rho_t} \beta_{mk}^d}{\tau_t^d \rho_t \beta_{mk}^d + 1}$ and $c_{ml}^u = \frac{\sqrt{\tau_t^u \rho_t} \beta_{ml}^u}{\tau_t^u \rho_t \beta_{ml}^u + 1}$. The estimation error vectors are defined as $\mathbf{e}_{ml}^u \triangleq \mathbf{g}_{ml}^u - \hat{\mathbf{g}}_{ml}^u$ and $\mathbf{e}_{mk}^d \triangleq \mathbf{g}_{mk}^d - \hat{\mathbf{g}}_{mk}^d$. With MMSE channel estimation, $\hat{\mathbf{g}}_{mk}^d$, \mathbf{e}_{mk}^d and $\hat{\mathbf{g}}_{ml}^u$, \mathbf{e}_{ml}^u are mutually independent and their individual terms are i.i.d. with pdf $\mathcal{CN}(0, \gamma_{mk}^d)$, $\mathcal{CN}(0, \beta_{mk}^d - \gamma_{mk}^d)$, $\mathcal{CN}(0, \gamma_{ml}^u)$, $\mathcal{CN}(0, \beta_{ml}^u - \gamma_{ml}^u)$ respectively, with $\gamma_{mk}^d = \frac{\tau_t^d \rho_t (\beta_{mk}^d)^2}{\tau_t^d \rho_t \beta_{mk}^d + 1}$ and $\gamma_{ml}^u = \frac{\tau_t^u \rho_t (\beta_{ml}^u)^2}{\tau_t^u \rho_t \beta_{ml}^u + 1}$ [5], [11]. After channel estimation, data transmission starts simultaneously on downlink and uplink.

Transmission model: An objective of this work is to derive a SE lower bound for FD CF mMIMO systems, where the M APs serve K_u uplink UEs and K_d downlink UEs simultaneously on the same spectral resource. We note that for the FD CF mMIMO systems, unlike the HD CF mMIMO systems [2], [8], [9], uplink and downlink transmissions interfere to cause UDI and inter-/intra-AP interferences. Further, unlike existing FD CF mMIMO literature [5], [6], [14], we consider a limited-capacity fronthaul. It is critical to model and analyze the UDI and inter-/intra-AP interferences and limited-capacity impairments while deriving the lower bound.

1) *Downlink data transmission:* The CPU chooses a message symbol s_k^d for the k th downlink UE, which is distributed as $\mathcal{CN}(0, 1)$. It intends to send this symbol to the m th AP via the limited-capacity fronthaul link. Before doing that, it multiplies s_k^d with a power-control coefficient η_{mk} , and then quantizes the resulting signal. The m th AP, due to its limited fronthaul capacity,

is allowed to serve only a subset $\kappa_{dm} \subset \{1, \dots, K_d\}$ of downlink users, an aspect which is discussed later in Section II-2. The CPU consequently sends downlink symbols for UEs in the set κ_{dm} to the m th AP, which uses MMSE channel estimates to perform MRT precoding. The transmit signal of the m th AP is therefore given as follows

$$\mathbf{x}_m^d = \sqrt{\rho_d} \sum_{k \in \kappa_{dm}} (\hat{\mathbf{g}}_{mk}^d)^* \mathcal{Q}(\sqrt{\eta_{mk}} s_k^d) = \sqrt{\rho_d} \sum_{k \in \kappa_{dm}} (\hat{\mathbf{g}}_{mk}^d)^* (\tilde{a} \sqrt{\eta_{mk}} s_k^d + \varsigma_{mk}^d). \quad (1)$$

Here ρ_d is the normalized maximum transmit SNR at each AP. The function $\mathcal{Q}(\cdot)$ denotes the quantization operation, which is modeled as a multiplicative attenuation, \tilde{a} , and an additive distortion, ς_{mk}^d , for the k th downlink UE in the fronthaul link between the CPU and the m th AP [8], [12]. We have, from Appendix A, $\mathbb{E}\{(\varsigma_{mk}^d)^2\} = (\tilde{b} - \tilde{a}^2) \mathbb{E}\{|\sqrt{\eta_{mk}} s_k^d|^2\} = (\tilde{b} - \tilde{a}^2) \eta_{mk}$, where the scalar constants \tilde{a} and \tilde{b} depend on the number of fronthaul quantization bits.

The m th AP must satisfy the average transmit SNR constraint, i.e., $\mathbb{E}\{\|\mathbf{x}_m^d\|^2\} \leq \rho_d$. Using the expression of \mathbf{x}_m^d from (1), and the above expression of quantization error variance, $\mathbb{E}\{(\varsigma_{mk}^d)^2\}$, the constraint can be simplified as follows

$$\rho_d \tilde{b} \sum_{k \in \kappa_{dm}} \eta_{mk} \mathbb{E}\{\|\hat{\mathbf{g}}_{mk}^d\|^2\} \leq \rho_d \Rightarrow \tilde{b} \sum_{k \in \kappa_{dm}} \gamma_{mk}^d \eta_{mk} \leq \frac{1}{N_t}. \quad (2)$$

The k th downlink UE receives its desired message signal from a subset of all APs, denoted as $\mathcal{M}_k^d \subset \{1, \dots, M\}$, along with various interference and distortion components, as follows

$$\begin{aligned} r_k^d &= \sum_{m=1}^M (\mathbf{g}_{mk}^d)^T \mathbf{x}_m^d + \sum_{l=1}^{K_u} h_{kl} x_l^u + w_k^d \\ &= \underbrace{\tilde{a} \sqrt{\rho_d} \sum_{m \in \mathcal{M}_k^d} \sqrt{\eta_{mk}} (\mathbf{g}_{mk}^d)^T (\hat{\mathbf{g}}_{mk}^d)^* s_k^d}_{\text{message signal}} + \underbrace{\tilde{a} \sqrt{\rho_d} \sum_{m=1}^M \sum_{q \in \kappa_{dm} \setminus k} \sqrt{\eta_{mq}} (\mathbf{g}_{mk}^d)^T (\hat{\mathbf{g}}_{mq}^d)^* s_q^d}_{\text{multi-UE interference, MUI}_k^d} \\ &\quad + \underbrace{\sum_{l=1}^{K_u} h_{kl} x_l^u}_{\text{uplink downlink interference, UDI}_k^d} + \underbrace{\sqrt{\rho_d} \sum_{m=1}^M \sum_{q \in \kappa_{dm}} (\mathbf{g}_{mk}^d)^T (\hat{\mathbf{g}}_{mq}^d)^* \varsigma_{mq}^d}_{\text{total quantization distortion, TQD}_k^d} + \underbrace{w_k^d}_{\text{AWGN at receiver}}. \end{aligned} \quad (3)$$

The m th AP serves the k th downlink UE iff $k \in \kappa_{dm} \Leftrightarrow m \in \mathcal{M}_k^d$. Here x_l^u is the transmit signal of the l th uplink UE, which is modelled next.

2) *Uplink data transmission:* The K_u uplink UEs also simultaneously transmit to all M APs on the same spectral resource as that of the K_d downlink UEs. The l th uplink UE transmits its signal $x_l^u = \sqrt{\rho_u \theta_l} s_l^u$ with s_l^u being its message symbol with pdf $\mathcal{CN}(0, 1)$, ρ_u being the maximum uplink transmit SNR and θ_l being the power control coefficient. To satisfy the average

SNR constraint, $\mathbb{E}\{|x_l^u|^2\} \leq \rho_u$, the l th uplink UE satisfies the following constraint

$$0 \leq \theta_l \leq 1. \quad (4)$$

The FD APs not only receive uplink UE signals but also their own downlink transmit signals and that of the other APs, referred to as intra-AP and inter-AP interference, respectively. Using (1), the received uplink signal at the m th AP is expressed as

$$\begin{aligned} \mathbf{y}_m^u &= \sum_{l=1}^{K_u} \mathbf{g}_{ml}^u x_l^u + \sum_{i=1}^M \mathbf{H}_{mi} \mathbf{x}_i^d + \mathbf{w}_m^u \\ &= \sqrt{\rho_u} \sum_{l=1}^{K_u} \mathbf{g}_{ml}^u \sqrt{\theta_l} s_l^u + \sqrt{\rho_d} \sum_{i=1}^M \sum_{k \in \kappa_{di}} \mathbf{H}_{mi} (\hat{\mathbf{g}}_{ik}^d)^* (\tilde{a} \sqrt{\eta_{ik}} s_k^d + \varsigma_{ik}^d) + \mathbf{w}_m^u. \end{aligned} \quad (5)$$

Here $\mathbf{w}_m^u \in \mathbb{C}^{N_r \times 1}$ is the additive receiver noise at the m th AP with i.i.d. entries $\sim \mathcal{CN}(0, 1)$.

The intra and inter-AP interference channels vary extremely slowly and thus can be estimated with very low pilot overhead [6]. The receive antenna array of each AP, with estimated channel, can only partially mitigate the intra- and inter-AP interference [5], [6]. The residual intra-/inter-AP interference (RI) channel $\mathbf{H}_{mi} \in \mathbb{C}^{N_r \times N_t}$ is modeled as Rayleigh-faded with i.i.d. entries $\sim \mathcal{CN}(0, \gamma_{\text{RI}, mi})$ [4]–[6], [17]. Here $\gamma_{\text{RI}, mi} \triangleq \beta_{\text{RI}, mi} \gamma_{\text{RI}}$, with $\beta_{\text{RI}, mi}$ being the large scale fading coefficient from the i th AP to the m th AP, and γ_{RI} being the RI power after its suppression. The m th AP receives the signals from all the uplink UEs, and performs MRC for the l th uplink UE with $(\hat{\mathbf{g}}_{ml}^u)^H$. Due to its limited fronthaul: i) AP quantizes the combined signal before sending it to CPU; ii) as discussed in detail later in Section II-2, the CPU receives contributions for the l th uplink UE only from the subset of APs serving it, denoted as $\mathcal{M}_l^u \subset \{1, \dots, M\}$. Using (5), the signal received by the CPU for the l th uplink UE is expressed as

$$\begin{aligned} r_l^u &= \sum_{m \in \mathcal{M}_l^u} \mathcal{Q}((\hat{\mathbf{g}}_{ml}^u)^H \mathbf{y}_m^u) = \underbrace{\tilde{a} \sum_{m \in \mathcal{M}_l^u} \sqrt{\rho_u} \sqrt{\theta_l} (\hat{\mathbf{g}}_{ml}^u)^H \mathbf{g}_{ml}^u s_l^u}_{\text{message signal}} + \underbrace{\tilde{a} \sum_{m \in \mathcal{M}_l^u} \sum_{\substack{q=1 \\ q \neq l}}^{K_u} \sqrt{\rho_u} \sqrt{\theta_q} (\hat{\mathbf{g}}_{ml}^u)^H \mathbf{g}_{mq}^u s_q^u}_{\text{multi-UE interference, MUI}_l^u} \\ &+ \underbrace{\tilde{a} \sum_{m \in \mathcal{M}_l^u} \sum_{i=1}^M \sqrt{\rho_d} \sum_{k \in \kappa_{di}} (\hat{\mathbf{g}}_{ml}^u)^H \mathbf{H}_{mi} (\hat{\mathbf{g}}_{ik}^d)^* (\tilde{a} \sqrt{\eta_{ik}} s_k^d + \varsigma_{ik}^d)}_{\text{residual interference (intra-AP and inter-AP), RI}_l^u} + \underbrace{\tilde{a} \sum_{m \in \mathcal{M}_l^u} (\hat{\mathbf{g}}_{ml}^u)^H \mathbf{w}_m^u}_{\text{AWGN at APs, N}_l^u} + \underbrace{\sum_{m \in \mathcal{M}_l^u} \varsigma_{ml}^u}_{\text{total quantization distortion, TQD}_l^u}. \end{aligned} \quad (6)$$

We denote the subset of uplink UEs served by the m th AP as $\kappa_{um} \subset \{1, \dots, K_u\}$. The m th AP serves the l th uplink UE iff $l \in \kappa_{um} \Leftrightarrow m \in \mathcal{M}_l^u$. The quantization operation $\mathcal{Q}(\cdot)$ is mathematically modeled using constant attenuation \tilde{a} , and additive distortion ς_{ml}^u which, as shown

in Appendix A, has power $\mathbb{E}\{(\varsigma_{ml}^u)^2\} = (\tilde{b} - \tilde{a}^2)\mathbb{E}\left\{|(\mathbf{g}_{ml}^u)^H \mathbf{y}_m|^2\right\}$.

Quantization, limited fronthaul and AP selection: The fronthaul between the m th AP and the CPU uses ν_m bits to quantize the real and imaginary parts of transmit signal of the m th downlink UE and the uplink receive signal after MRC i.e., $\sqrt{\eta_{mk}}s_k^d$, and $(\hat{\mathbf{g}}_{ml}^u)^H \mathbf{y}_m^u$, respectively. Due to the limited-capacity fronthaul, the m th AP serves only $K_{um}(\triangleq |\kappa_{um}|)$ and $K_{dm}(\triangleq |\kappa_{dm}|)$ UEs on the uplink and downlink, respectively [8], [12]. For each UE, we recall that there are $(\tau_c - \tau_t)$ data samples in each coherence interval of duration T_c . The fronthaul data rate between the m th AP and the CPU, in bps (bits per second), is

$$R_{\text{fh},m} = \frac{2\nu_m(K_{dm} + K_{um})(\tau_c - \tau_t)}{T_c}. \quad (7)$$

The fronthaul link between the m th AP and the CPU has capacity $C_{\text{fh},m}$ which implies that

$$R_{\text{fh},m} \leq C_{\text{fh},m} \Rightarrow \nu_m \cdot (K_{um} + K_{dm}) \leq \frac{C_{\text{fh},m}T_c}{2(\tau_c - \tau_t)}. \quad (8)$$

We propose the following lemma where we consider a *proportionally fair* approach to calculate K_{dm} and K_{um} . We set them *in proportion to* the total downlink and uplink UEs, respectively.

Lemma 1. The maximum number of uplink and downlink UEs served by the m th AP when connected via a limited optical fronthaul to the CPU with capacity $C_{\text{fh},m}$ are given as

$$\bar{K}_{dm} = \left\lfloor \frac{K_d}{(K_u + K_d)} \frac{C_{\text{fh},m}T_c}{4(\tau_c - \tau_t)\nu_m} \right\rfloor, \bar{K}_{um} = \left\lfloor \frac{K_u}{(K_u + K_d)} \frac{C_{\text{fh},m}T_c}{4(\tau_c - \tau_t)\nu_m} \right\rfloor. \quad (9)$$

Proof: Let \bar{K}_{um} and \bar{K}_{dm} denote the maximum number of uplink and downlink UEs served by the m th AP. We consider $\bar{K}_{um} \propto K_u$ and $\bar{K}_{dm} \propto K_d$ for proportional fairness on the uplink and downlink. Using (8), we get,

$$\bar{K}_{dm} \leq \frac{K_d}{(K_u + K_d)} \frac{C_{\text{fh},m}T_c}{2(\tau_c - \tau_t)\nu_m}, \bar{K}_{um} \leq \frac{K_u}{(K_u + K_d)} \frac{C_{\text{fh},m}T_c}{2(\tau_c - \tau_t)\nu_m}.$$

The lemma follows directly from the definition of floor function $\lfloor \cdot \rfloor$. ■

Using the maximum limits obtained in (9), we assign $K_{um} = \min\{K_u, \bar{K}_{um}\}$ and $K_{dm} = \min\{K_d, \bar{K}_{dm}\}$. We see that the constraint imposed in (8) is similar to a UE-centric (UC) CF mMIMO system, wherein each UE is served by a subset of the APs [3]. We now define the procedure for AP selection to obtain the best subset of APs to serve each uplink and downlink UE, while satisfying (8). For this, we extend the procedure in [8] for a FD system as follows:

- The m th AP sorts the uplink and downlink UEs connected to it in descending order based on their channel gains (β_{ml}^u and β_{mk}^d , respectively) and chooses K_{um} uplink UEs and K_{dm} downlink UEs, with the largest channel gains, to populate the sets κ_{um} and κ_{dm} , respectively.

- For the l th uplink UE and the k th downlink UE, we populate the sets \mathcal{M}_l^u and \mathcal{M}_k^d , respectively, using the axioms $l \in \kappa_{um} \Leftrightarrow m \in \mathcal{M}_l^u$ and $k \in \kappa_{dm} \Leftrightarrow m \in \mathcal{M}_k^d$.
- If an uplink or downlink UE is found with no serving AP, we use the procedure in Algorithm 1 to assign it the AP with the best channel conditions, while satisfying (8).

Algorithm 1: Fair AP selection for disconnected uplink and downlink UEs

```

1 for  $k \leftarrow 1$  to  $K_d$  do
2   if  $\mathcal{M}_k^d = \emptyset$  then
     Sort the APs in descending order of channel gains,  $\beta_{mk}^d$ , and find the AP  $n$  with the largest channel gain.
     For this  $n$ th AP, sort downlink UEs in  $\kappa_{dn}$  in descending order of channel gains and find the  $q$ th downlink UE
     with minimum channel gain and at least one more connected AP.
     Remove the  $q$ th downlink UE from the set  $\kappa_{dn}$  and add the  $k$ th downlink UE to it.
3 Repeat the same procedure for all the uplink UEs  $l = 1$  to  $K_u$ .

```

III. ACHIEVABLE SPECTRAL EFFICIENCY

We now derive the ergodic SE for the k th downlink UE and the l th uplink UE, denoted respectively as \bar{S}_k^d and \bar{S}_l^u . The AP employs MRC/MRT in the uplink/downlink and optimal uniform fronthaul quantization. The ergodic SE expressions are calculated using (3) and (6), as

$$\bar{S}_\phi^\varepsilon = \left(\frac{\tau_c - \tau_t}{\tau_c} \right) \mathbb{E} \left\{ \log_2 \left(1 + \frac{P_\phi^\varepsilon}{I_\phi^\varepsilon + (\sigma_{\phi,0}^\varepsilon)^2} \right) \right\}, \text{ where} \quad (10)$$

$$P_\phi^\varepsilon = \left| \tilde{a} \sum_{m \in \mathcal{M}_\phi^\varepsilon} \sqrt{\rho_\varepsilon} \sqrt{v_{m\phi}^\varepsilon} (\hat{\mathbf{g}}_{m\phi}^\varepsilon)^H \mathbf{g}_{m\phi}^\varepsilon s_\phi^\varepsilon \right|^2, (\sigma_{l,0}^u)^2 = \left| \tilde{a} \sum_{m \in \mathcal{M}_l^u} (\hat{\mathbf{g}}_{ml}^u)^H \mathbf{w}_m^u \right|^2, (\sigma_{k,0}^d)^2 = |w_k^d|^2,$$

$$I_l^u = \left| \tilde{a} \sum_{m \in \mathcal{M}_l^u} \sum_{\substack{q=1 \\ q \neq l}}^{K_u} \sqrt{\rho_u} \sqrt{\theta_q} (\hat{\mathbf{g}}_{ml}^u)^H \mathbf{g}_{mq}^u s_q^u \right|^2$$

$$+ \left| \tilde{a} \sum_{m \in \mathcal{M}_l^u} \sum_{i=1}^M \sqrt{\rho_d} \sum_{k \in \kappa_{di}} (\hat{\mathbf{g}}_{ml}^u)^H \mathbf{H}_{mi} (\hat{\mathbf{g}}_{ik}^d)^* (\tilde{a} \sqrt{\eta_{ik}} s_k^d + \varsigma_{ik}^d) \right|^2 + \left| \sum_{m \in \mathcal{M}_l^u} \varsigma_{ml}^u \right|^2,$$

$$I_k^d = \left| \sum_{l=1}^{K_u} h_{kl} \sqrt{\rho_u} \theta_l s_l^u \right|^2 + \left| \tilde{a} \sqrt{\rho_d} \sum_{m=1}^M \sum_{q \in \kappa_{dm} \setminus k} \sqrt{\eta_{mq}} (\mathbf{g}_{mk}^d)^T (\hat{\mathbf{g}}_{mq}^d)^* s_q^d \right|^2$$

$$+ \left| \sqrt{\rho_d} \sum_{m=1}^M \sum_{q \in \kappa_{dm}} (\mathbf{g}_{mk}^d)^T (\hat{\mathbf{g}}_{mq}^d)^* \varsigma_{mq}^d \right|^2,$$

are signal, noise and interference powers, respectively, for the l th uplink and k th downlink UEs.

We use $\varepsilon \triangleq \{d, u\}$ to denote downlink and uplink, respectively; $\phi \triangleq \{k, l\}$ to denote k th downlink UE and l th uplink UE, respectively; and $v_{m\phi}^\varepsilon \triangleq \{\eta_{mk} \text{ for } \phi = k, \theta_l \text{ for } \phi = l\}$. The expectation outside logarithm in the SE expressions in (10) is mathematically intractable, and it

is difficult to simplify them further [2], [5], [8]. We, similar to [2], employ use-and-then-forget (UatF) technique to derive SE lower bounds. To use UatF, we rewrite the received signal at the CPU for the l th uplink UE in (6), and at the k th downlink UE in (3), as

$$r_\phi^\varepsilon = \underbrace{\tilde{a} \sum_{m \in \mathcal{M}_\phi^\varepsilon} \sqrt{\rho_\varepsilon} \sqrt{v_{m\phi}^\varepsilon} \mathbb{E}\{(\hat{\mathbf{g}}_{m\phi}^\varepsilon)^H \mathbf{g}_{m\phi}^\varepsilon\}}_{\text{desired signal, DS}_\phi^\varepsilon} s_\phi^\varepsilon + n_\phi^\varepsilon, \quad (11)$$

where the effective additive noise terms n_ϕ^ε are expressed as follows:

$$\begin{aligned} n_l^u &= \underbrace{\tilde{a} \sqrt{\rho_u} \sqrt{\theta_l} \sum_{m \in \mathcal{M}_l^u} ((\hat{\mathbf{g}}_{ml}^u)^H \mathbf{g}_{ml}^u - \mathbb{E}\{(\hat{\mathbf{g}}_{ml}^u)^H \mathbf{g}_{ml}^u\}) s_l^u}_{\text{beamforming uncertainty, BU}_l^u} + \underbrace{\tilde{a} \sum_{m \in \mathcal{M}_l^u} \sum_{\substack{q=1 \\ q \neq l}}^{K_u} \sqrt{\rho_u} \sqrt{\theta_q} (\hat{\mathbf{g}}_{ml}^u)^H \mathbf{g}_{mq}^u s_q^u}_{\text{MUI}_l^u} \\ &+ \underbrace{\tilde{a} \sum_{m \in \mathcal{M}_l^u} \sum_{i=1}^M \sqrt{\rho_d} \sum_{k \in \kappa_{di}} (\hat{\mathbf{g}}_{ml}^u)^H \mathbf{H}_{mi} (\hat{\mathbf{g}}_{ik}^d)^* (\tilde{a} \sqrt{\eta_{ik}} s_k^d + \varsigma_{ik}^d)}_{\text{RI}_l^u} + \underbrace{\tilde{a} \sum_{m \in \mathcal{M}_l^u} (\hat{\mathbf{g}}_{ml}^u)^H \mathbf{w}_m^u}_{N_l^u} + \underbrace{\sum_{m \in \mathcal{M}_l^u} \varsigma_{ml}^u}_{\text{TQD}_l^u}, \quad (12) \\ n_k^d &= \underbrace{\tilde{a} \sqrt{\rho_d} \sum_{m \in \mathcal{M}_k^d} \sqrt{\eta_{mk}} ((\mathbf{g}_{mk}^d)^T (\hat{\mathbf{g}}_{mk}^d)^* - \mathbb{E}\{(\mathbf{g}_{mk}^d)^T (\hat{\mathbf{g}}_{mk}^d)^*\}) s_k^d}_{\text{beamforming uncertainty, BU}_k^d} + \underbrace{\sqrt{\rho_u} \sum_{l=1}^{K_u} h_{kl} \sqrt{\theta_l} s_l^u}_{\text{UDI}_k^d} \\ &+ \underbrace{\tilde{a} \sqrt{\rho_d} \sum_{m=1}^M \sum_{q \in \kappa_{dm} \setminus k} \sqrt{\eta_{mq}} (\mathbf{g}_{mk}^d)^T (\hat{\mathbf{g}}_{mq}^d)^* s_q^d}_{\text{MUI}_k^d} + \underbrace{\sqrt{\rho_d} \sum_{m=1}^M \sum_{q \in \kappa_{dm}} (\mathbf{g}_{mk}^d)^T (\hat{\mathbf{g}}_{mq}^d)^* \varsigma_{mq}^d + w_k^d}_{\text{TQD}_k^d}. \quad (13) \end{aligned}$$

The term $\text{DS}_\phi^\varepsilon$ in (11) denotes the desired signal received over the channel mean, and the term $\text{BU}_\phi^\varepsilon$ in (12)-(13) denotes beamforming uncertainty i.e., the signal received over deviation of channel from mean. It is easy to see that n_ϕ^ε are uncorrelated with their respective $\text{DS}_\phi^\varepsilon$ terms. We, similar to [5], treat them as worst-case additive Gaussian noise, an approximation which is tight for mMIMO systems [5]. Using (11)-(13), we next derive an achievable SE lower bound.

Theorem 1. An achievable lower bound to the SE for the k th downlink UE with MRT and the l th uplink UE with MRC can be expressed respectively as

$$S_k^d(\boldsymbol{\eta}, \boldsymbol{\Theta}, \boldsymbol{\nu}) = \tau_f \log_2 \left(1 + \frac{(\sum_{m \in \mathcal{M}_k^d} A_{mk}^d \sqrt{\eta_{mk}})^2}{\sum_{m=1}^M \sum_{q \in \kappa_{dm}} B_{kmq}^d \eta_{mq} + \sum_{l=1}^{K_u} D_{kl}^d \theta_l + 1} \right), \quad (14)$$

$$S_l^u(\boldsymbol{\eta}, \boldsymbol{\Theta}, \boldsymbol{\nu}) = \tau_f \log_2 \left(1 + \frac{A_l^u \theta_l}{\sum_{q=1}^{K_u} B_{lq}^u \theta_q + \sum_{i=1}^M \sum_{k \in \kappa_{di}} D_{lik}^u \eta_{ik} + E_l^u \theta_l + F_l^u} \right), \quad (15)$$

where $\tau_f = \left(\frac{\tau_c - \tau_t}{\tau_c}\right)$, $A_l^u = \tilde{a}^2 N_r^2 \rho_u \left(\sum_{m \in \mathcal{M}_l^u} \gamma_{ml}^u\right)^2$, $B_{lq}^u = \tilde{b} N_r \rho_u \sum_{m \in \mathcal{M}_l^u} \gamma_{ml}^u \beta_{mq}^u$, $D_{lik}^u = \tilde{b}^2 N_r N_t \rho_d \gamma_{ik}^d \sum_{m \in \mathcal{M}_l^u} \gamma_{ml}^u \beta_{RI,mi} \gamma_{RI}$, $E_l^u = (\tilde{b} - \tilde{a}^2) N_r^2 \rho_u \sum_{m \in \mathcal{M}_l^u} (\gamma_{ml}^u)^2$, $F_l^u = \tilde{b} N_r \sum_{m \in \mathcal{M}_l^u} \gamma_{ml}^u$, $A_{mk}^d = \tilde{a} N_t \sqrt{\rho_d} \gamma_{mk}^d$, $B_{kmq}^d = \tilde{b} N_t \rho_d \beta_{mk}^d \gamma_{mq}^d$ and $D_{kl}^d = \rho_u \tilde{\beta}_{kl}$. Here $\boldsymbol{\eta} \triangleq \{\eta_{mk}\} \in \mathbb{C}^{M \times K_d}$, $\boldsymbol{\Theta} \triangleq \{\theta_l\} \in \mathbb{C}^{K_u \times 1}$ and $\boldsymbol{\nu} \triangleq \{\nu_m\} \in \mathbb{C}^{M \times 1}$ are the variables on which the SE is dependent. We recall from Section II that \tilde{a} and \tilde{b} in (14)-(15) depend on the number of quantization bits, $\boldsymbol{\nu}$.

Proof: Refer to the supporting document [22]. This proof simplifies uplink downlink interference UDI_k^d and residual intra-/inter-AP interference, RI_l^u . The SE expressions are functions of large scale fading coefficients, γ_{mk}^d and γ_{ml}^u , which we will use to optimize WSEE. *This is unlike [14] which requires instantaneous channel while optimizing SE-GEE metric.* ■

Remark 1. MRC/MRT has tractable SE expression that depend solely on large-scale channel statistics, which remain constant over *hundreds* of coherence intervals [23] *This is critical for optimization discussed next which use these SE expressions, and will thus be solved infrequently.* This is in contrast to zero-forcing designs which yield better SE but not tractable SE expressions [24]. Further, MRC/MRT can be implemented in a distributed fashion with low complexity.

IV. TWO-LAYER DECENTRALIZED WSEE OPTIMIZATION FOR FD CF MMIMO

We now devise a decentralized algorithm which maximizes WSEE by calculating the optimal downlink and uplink power control coefficients $\boldsymbol{\eta}^*$ and $\boldsymbol{\Theta}^*$, respectively. We use “two-layered” approach to decompose WSEE maximization into a sequential process with two distinct individual steps, each of which is called a “layer”. The first layer simplifies the non-convex WSEE maximization into a successive convex approximation (SCA) setting. Its output is a generalized convex program (GCP) which needs to be solved iteratively for the optimal solution. The second layer optimally solves above GCP, either centrally through standard interior-point approaches or decentrally using ADMM method. The proposed procedure is outlined in Algorithm 2.

Algorithm 2: Two-layer decentralized WSEE maximization

- 1 *AP selection:* Select APs that serve each UE while satisfying limited fronthaul constraints.
 - 2 *SCA framework (first layer):* Apply a series of transformations and approximations to recast the non-convex WSEE maximization using successive convex approximation (SCA) framework. The output of first layer is a GCP.
 - 3 *Decentralized ADMM approach (second layer):* Introduce global and local variables to decouple the problem into multiple sub-problems. Each sub-problem is solved at a distributed (or “D”) server, whose solutions are coordinated to obtain the global solution at the central (or “C”) server. This procedure is implemented using ADMM.
-

We use $\varepsilon \triangleq \{d, u\}$ for the downlink and uplink, respectively; $\phi \triangleq \{k, l\}$ for the k th downlink UE and l th uplink UE, respectively; and first define the individual EE for each UE as $\text{EE}_\phi^\varepsilon = \frac{B \cdot S_\phi^\varepsilon}{p_\phi^\varepsilon}$

[16], where B is the system bandwidth, and p_ϕ^ε denotes the power consumed by each UE. The fronthaul links consume power for both downlink and uplink transmission. The APs consume power while transmitting data to the downlink UEs, and the uplink UEs consume power while transmitting their data. The power consumed by the system to transmit data to the k th downlink UE and the power consumed by the l th uplink UE are given respectively as [12], [14]

$$p_k^d = P_{\text{fix}} + N_t \rho_d N_0 \sum_{m \in \mathcal{M}_k^d} \frac{1}{\alpha_m} \gamma_{mk}^d \eta_{mk} + P_{\text{tc},k}^d, \text{ and } p_l^u = P_{\text{fix}} + \rho_u N_0 \frac{1}{\alpha_l'} \theta_l + P_{\text{tc},l}^u. \quad (16)$$

Here α_m and α_l' are power amplifier efficiencies at the m th AP and the l th uplink UE respectively [5], N_0 is the noise power and $P_{\text{tc},k}^d$ and $P_{\text{tc},l}^u$ are the powers required to run the transceiver chains at each antenna of the k th downlink UE and the l th uplink UE, respectively. The power consumed by the AP transceiver chains and the fronthaul between APs and CPU:

$$P_{\text{fix}} = \frac{1}{(K_u + K_d)} \sum_{m=1}^M \left(P_{0,m} + (N_t + N_r) P_{\text{tc},m} + P_{\text{ft}} \frac{R_{\text{fh},m}}{C_{\text{fh},m}} \right). \quad (17)$$

Here $P_{\text{tc},m}$ is the power required to run the transceiver chains at each antenna of the m th AP. The fronthaul power consumption for the m th AP has a fixed component, $P_{0,m}$, and a traffic-dependent component, which attains a maximum value of P_{ft} at full capacity $C_{\text{fh},m}$. The term $R_{\text{fh},m}$, given in (7), is the fronthaul data rate of the m th AP.

The WSEE is now defined as the weighted sum of individual EEs of different users [15], as

$$\text{WSEE} = \sum_{k=1}^{K_d} w_k^d \text{EE}_k^d + \sum_{l=1}^{K_u} w_l^u \text{EE}_l^u \triangleq B \left(\sum_{k=1}^{K_d} w_k^d \frac{S_k^d(\boldsymbol{\eta}, \boldsymbol{\Theta}, \boldsymbol{\nu})}{p_k^d(\boldsymbol{\eta}, \boldsymbol{\nu})} + \sum_{l=1}^{K_u} w_l^u \frac{S_l^u(\boldsymbol{\eta}, \boldsymbol{\Theta}, \boldsymbol{\nu})}{p_l^u(\boldsymbol{\Theta}, \boldsymbol{\nu})} \right), \quad (18)$$

where w_ϕ^ε are weights assigned to the UEs to account for their heterogeneous EE requirements. The WSEE metric can prioritize the EE requirements of individual UEs by assigning them different weights [16], [17]. For example, it could assign a higher weight to a UE that is more energy-scarce. The WSEE maximization problem can now be formulated as follows

$$\begin{aligned} \mathbf{P1} : \max_{\boldsymbol{\eta}, \boldsymbol{\Theta}, \boldsymbol{\nu}} \quad & B \left(\sum_{k=1}^{K_d} w_k^d \frac{S_k^d(\boldsymbol{\eta}, \boldsymbol{\Theta}, \boldsymbol{\nu})}{p_k^d(\boldsymbol{\eta}, \boldsymbol{\nu})} + \sum_{l=1}^{K_u} w_l^u \frac{S_l^u(\boldsymbol{\eta}, \boldsymbol{\Theta}, \boldsymbol{\nu})}{p_l^u(\boldsymbol{\Theta}, \boldsymbol{\nu})} \right) \\ \text{s.t.} \quad & S_k^d(\boldsymbol{\eta}, \boldsymbol{\Theta}, \boldsymbol{\nu}) \geq S_{ok}^d, S_l^u(\boldsymbol{\eta}, \boldsymbol{\Theta}, \boldsymbol{\nu}) \geq S_{ol}^u, \end{aligned} \quad (19a)$$

$$R_{\text{fh},m} \leq C_{\text{fh},m}, (2), (4). \quad (19b)$$

The quality-of-service (QoS) constraints in (19a) guarantee a minimum SE, denoted by the constants S_{ok}^d and S_{ol}^u , for each downlink and uplink UE respectively. The first constraint in (19b) ensures that the fronthaul transmission rate for all APs is within the capacity limit. We observe

that the number of quantization bits ν , if included in problem **P1**, will make it a difficult-to-solve integer optimization problem [8], [12], [25]. We therefore solve it to optimize the power control coefficients $\{\eta, \Theta\}$, by fixing ν such that it satisfies the first constraint in (19b) [8], [12], and numerically investigate ν in Section V. We omit the constant B and reformulate **P1** as follows

$$\begin{aligned} \mathbf{P2} : \max_{\eta, \Theta} \quad & \sum_{k=1}^{K_d} w_k^d \frac{S_k^d(\eta, \Theta)}{p_k^d(\eta)} + \sum_{l=1}^{K_u} w_l^u \frac{S_l^u(\eta, \Theta)}{p_l^u(\Theta)} \\ \text{s.t.} \quad & S_k^d(\eta, \Theta) \geq S_{ok}^d, \quad S_l^u(\eta, \Theta) \geq S_{ol}^u, \\ & (2), (4). \end{aligned} \quad (20)$$

The objective in **P2** is a sum of ratios, each of which is a PC function (concave-over-linear) of power control coefficients $\{\eta, \Theta\}$. It is, therefore, not guaranteed to be a PC function and Dinkelbach's algorithm cannot be applied to maximize it [15]. This makes it a much harder objective to optimize as opposed to the more commonly studied GEE metric, which is a PC function [15] and has been investigated for CF mMIMO systems [11]–[14].

We now maximize WSEE centrally and decentrally using a two-layered approach. The first layer comprises an SCA framework, which formulates a GCP by approximating the non-convex objective and constraints in **P2** as convex. In the second layer, the approximate GCP formed in the n th SCA iteration is either solved centrally or decentrally using ADMM. Since the approximate GCP obtained in the first layer, due to coupled optimization variables, is not in the standard ADMM form, we introduce their local and global versions. The sub-problems to update local variables are solved independently, and the local variables are coordinated to calculate the global solution [20], [21], [26]. The updation of variables and coordination continues till ADMM converges. The obtained solution is then used to formulate GCP for $(n+1)$ th SCA iteration.

A. SCA Framework

We now first linearize the non-convex objective in **P2** using epigraph transformation as [25]

$$\begin{aligned} \mathbf{P3} : \max_{\eta, \Theta, f^d, f^u} \quad & \sum_{k=1}^{K_d} w_k^d f_k^d + \sum_{l=1}^{K_u} w_l^u f_l^u \\ \text{s.t.} \quad & f_k^d \leq \frac{S_k^d(\eta, \Theta)}{p_k^d(\eta)}, \quad f_l^u \leq \frac{S_l^u(\eta, \Theta)}{p_l^u(\Theta)}, \\ & (2), (4), (20). \end{aligned} \quad (21)$$

Here $\mathbf{f}^\varepsilon \triangleq [f_1^\varepsilon \dots f_{K_\varepsilon}^\varepsilon] \in \mathbb{C}^{K_\varepsilon \times 1}$ are slack variables [25]. To approximate the non-convex constraints in (20) and (21) as convex, we substitute S_k^d and S_l^u from (14)–(15) and cross-multiply the

terms p_k^d, p_l^u and f_k^d, f_l^u in (21). We also introduce slack variables $\Psi^\varepsilon \triangleq [\Psi_1^\varepsilon, \dots, \Psi_{K_\varepsilon}^\varepsilon] \in \mathbb{C}^{K_\varepsilon \times 1}$, $\zeta^\varepsilon \triangleq [\zeta_1^\varepsilon, \dots, \zeta_{K_\varepsilon}^\varepsilon] \in \mathbb{C}^{K_\varepsilon \times 1}$ and equivalently cast **P3** as follows [15]

$$\begin{aligned} \mathbf{P4} : \quad & \max_{\eta, \Theta, f^d, f^u, \Psi^d, \Psi^u, \zeta^d, \zeta^u} \sum_{k=1}^{K_d} w_k^d f_k^d + \sum_{l=1}^{K_u} w_l^u f_l^u \\ \text{s.t.} \quad & p_k^d \leq \frac{(\Psi_k^d)^2}{f_k^d}, p_l^u \leq \frac{(\Psi_l^u)^2}{f_l^u}, \end{aligned} \quad (22a)$$

$$(\Psi_k^d)^2 \leq \tau_f \log_2(1 + \zeta_k^d), (\Psi_l^u)^2 \leq \tau_f \log_2(1 + \zeta_l^u), \quad (22b)$$

$$\zeta_k^d \leq \frac{(\sum_{m \in \mathcal{M}_k^d} A_{mk}^d \sqrt{\eta_{mk}})^2}{\sum_{m=1}^M \sum_{q \in \kappa_{dm}} B_{kmq}^d \eta_{mq} + \sum_{l=1}^{K_u} D_{kl}^d \theta_l + 1}, \quad (22c)$$

$$\zeta_l^u \leq \frac{A_l^u \theta_l}{\sum_{q=1}^{K_u} B_{lq}^u \theta_q + \sum_{i=1}^M \sum_{k \in \kappa_{di}} D_{lik}^u \eta_{ik} + E_l^u \theta_l + F_l^u}, \quad (22d)$$

$$\log_2(1 + \zeta_k^d) \geq S_{ok}^d / \tau_f, \log_2(1 + \zeta_l^u) \geq S_{ol}^u / \tau_f, \quad (22e)$$

(2), (4).

We introduce the variable $c_{mk} \triangleq \sqrt{\eta_{mk}}$ and denote $\mathbf{C} \triangleq \{c_{mk}\} \in \mathbb{C}^{M \times K_d}$ to remove concave terms in (22c) arising due to $\sqrt{\eta_{mk}}$ and facilitate its conversion into a convex constraint. We introduce additional slack variables $\lambda^\varepsilon \triangleq [\lambda_1^\varepsilon, \dots, \lambda_{K_\varepsilon}^\varepsilon] \in \mathbb{C}^{K_\varepsilon \times 1}$ to further simplify the non-convex constraints (22c)-(22d). We now cast **P4** equivalently as follows

$$\begin{aligned} \mathbf{P5} : \quad & \max_{C, \Theta, f^d, f^u, \Psi^d, \Psi^u, \zeta^d, \zeta^u, \lambda^d, \lambda^u} \sum_{k=1}^{K_d} w_k^d f_k^d + \sum_{l=1}^{K_u} w_l^u f_l^u \\ \text{s.t.} \quad & \sum_{m=1}^M \sum_{q \in \kappa_{dm}} B_{kmq}^d c_{mq}^2 + \sum_{l=1}^{K_u} D_{kl}^d \theta_l + 1 \leq \frac{(\lambda_k^d)^2}{\zeta_k^d}, \end{aligned} \quad (23a)$$

$$\sum_{q=1}^{K_u} B_{lq}^u \theta_q + \sum_{i=1}^M \sum_{k \in \kappa_{di}} D_{lik}^u c_{ik}^2 + E_l^u \theta_l + F_l^u \leq \frac{(\lambda_l^u)^2}{\zeta_l^u}, \quad (23b)$$

$$\lambda_k^d \leq \sum_{m \in \mathcal{M}_k^d} A_{mk}^d c_{mk}, (\lambda_l^u)^2 \leq A_l^u \theta_l, \quad (23c)$$

$$\lambda_k^d \geq 0, \tilde{b} \sum_{k \in \kappa_{dm}} \gamma_{mk}^d c_{mk}^2 \leq \frac{1}{N_t}, c_{mk} \geq 0, \quad (23d)$$

(22a), (22b), (22e), (4).

We note that **P5** has all convex constraints except (22a) and (23a)-(23b). Since a first-order Taylor approximation is a global under-estimator of a convex function [25], we now linearize

the right-hand side of these constraints. At the n th iteration, we substitute first-order Taylor approximate $\frac{f_1^2}{f_2} \geq 2\frac{f_1^{(n)}}{f_2^{(n)}}f_1 - \frac{(f_1^{(n)})^2}{(f_2^{(n)})^2}f_2 \triangleq \Lambda^{(n)}\left(\frac{f_1^2}{f_2}\right)$ and use (16) to recast **P5** into a GCP:

$$\begin{aligned} \mathbf{P6}: \quad & \max_{C, \Theta, f^d, f^u, \Psi^d, \Psi^u, \zeta^d, \zeta^u, \lambda^d, \lambda^u} \sum_{k=1}^{K_d} w_k^d f_k^d + \sum_{l=1}^{K_u} w_l^u f_l^u \\ \text{s.t.} \quad & \sum_{q=1}^{K_u} B_{lq}^u \theta_q + \sum_{i=1}^M \sum_{k \in \kappa_{di}} D_{lik}^u c_{ik}^2 + E_l^u \theta_l + F_l^u \leq \Lambda^{(n)}\left(\frac{(\lambda_l^u)^2}{\zeta_l^u}\right), \end{aligned} \quad (24a)$$

$$\sum_{m=1}^M \sum_{q \in \kappa_{dm}} B_{kmq}^d c_{mq}^2 + \sum_{l=1}^{K_u} D_{kl}^d \theta_l + 1 \leq \Lambda^{(n)}\left(\frac{(\lambda_k^d)^2}{\zeta_k^d}\right), \quad (24b)$$

$$P_{\text{fix}} + N_t \rho_d N_0 \sum_{m \in \mathcal{M}_k^d} \frac{1}{\alpha_m} \gamma_{mk}^d c_{mk}^2 + P_{\text{tc},k}^d \leq \Lambda^{(n)}\left(\frac{(\Psi_k^d)^2}{f_k^d}\right), \quad (24c)$$

$$P_{\text{fix}} + \rho_u N_0 \frac{1}{\alpha_l'} \theta_l + P_{\text{tc},l}^u \leq \Lambda^{(n)}\left(\frac{(\Psi_l^u)^2}{f_l^u}\right), \quad (24d)$$

(4), (22b), (22e), (23c), (23d).

We next provide a centralized SCA to solve **P6** in the second layer in Algorithm 3.

Algorithm 3: Centralized WSEE maximization algorithm

Input: i) Initialize power control coefficients $\{C, \Theta\}^{(1)}$ by allocating equal power to all downlink UEs being served and full power to all uplink UEs. Set $n = 1$.

ii) Initialize $\{f^d, f^u, \Psi^d, \Psi^u, \zeta^d, \zeta^u, \lambda^d, \lambda^u\}^{(1)}$ by replacing (23c), (24a)-(24b), (22b) and (24c)-(24d) by equality.

Output: Globally optimal power control coefficients $\{C, \Theta\}^*$

```

1 while  $\|r_{\text{SCA}}^{(n)}\| \leq \epsilon_{\text{SCA}}$  do
2   Solve P6 for the  $n$ th SCA iteration to obtain optimal variables,  $\{f^d, f^u, \Psi^d, \Psi^u, \zeta^d, \zeta^u, \lambda^d, \lambda^u, C, \Theta\}^{*,(n)}$ .
3   Assign the SCA iterates for the  $(n+1)$ th iteration,
    $\{f^d, f^u, \Psi^d, \Psi^u, \zeta^d, \zeta^u, \lambda^d, \lambda^u, C, \Theta\}^{(n+1)} = \{f^d, f^u, \Psi^d, \Psi^u, \zeta^d, \zeta^u, \lambda^d, \lambda^u, C, \Theta\}^{*,(n)}$ .

```

The SCA procedure converges when $\|r_{\text{SCA}}^{(n)}\| = \sqrt{\|C^{(n+1)} - C^{(n)}\|_F^2 + \|\Theta^{(n+1)} - \Theta^{(n)}\|^2}$ has a magnitude $\|r_{\text{SCA}}^{(n)}\| \leq \epsilon_{\text{SCA}}$, where ϵ_{SCA} is the convergence threshold.

Remark 2. Convergence of centralized algorithm: At the n th SCA iteration, **P6** is obtained from **P5** by applying first-order Taylor approximations to the constraints (22a) and (23a)-(23b). These approximations are of the form $\Lambda(x) \triangleq \frac{x_1^2}{x_2} \geq 2\frac{x_1^{(n)}}{x_2^{(n)}}x_1 - \left(\frac{x_1^{(n)}}{x_2^{(n)}}\right)^2 x_2 \triangleq \bar{\Lambda}(x, x^{(n)})$. It can be easily shown that **P6** is the *inner-approximation problem* for **P5**, where we replace each of the constraints (22a) and (23a)-(23b), denoted generally as $g_i(x) \leq 0, i = 1, 2, 3$, with a convex approximation of the form $\bar{g}_i(x, x^{(n)}) \leq 0, i = 1, 2, 3$. For each of the approximations, it can

be easily shown that the following properties hold [27]: i) $g_i(\mathbf{x}) \leq \bar{g}_i(\mathbf{x}, \mathbf{x}^{(n)})$ for all feasible \mathbf{x} ; ii) $g_i(\mathbf{x}^{(n)}) = \bar{g}_i(\mathbf{x}^n, \mathbf{x}^{(n)})$; and $\frac{\partial g_i(\mathbf{x}^{(n)})}{\partial x_j} = \frac{\partial \bar{g}_i(\mathbf{x}^n, \mathbf{x}^{(n)})}{\partial x_j}$, $j = 1, 2$. The constraints in **P6** also satisfy Slater's conditions [25]. This implies that Algorithm 3, by solving the inner-approximation problem, always converges to a KKT point of **P2** due to [27], [28].

B. Decentralized ADMM approach

We now use ADMM to solve **P6** decentrally in the second layer, an approach well-suited for CPUs with multiple distributed D-servers, connected via a central C-server [18], [19]. ADMM decomposes a central problem into multiple sub-problems, each of which is solved by a D-server locally and independently. The C-server combines the local solutions to obtain a global solution. We observe that the constraints in (24a)-(24b) couple the power control coefficients of different uplink and downlink UEs. We next introduce global variables for the power control coefficients at the C-server, with local copies at the D-servers to decouple **P6** into sub-problems for each UE [21]. We observe that the constraints in **P6** for the downlink and uplink UEs can be divided between downlink and uplink D-servers, respectively. The D-servers solve sub-problems defined for each downlink and uplink UE. We first define local feasible sets at the n th SCA iteration for them, which are denoted as $\mathcal{S}_k^{d,(n)}$ and $\mathcal{S}_l^{u,(n)}$, respectively. These sets are given as follows

$$\mathcal{S}_k^{d,(n)} = \left\{ f_k^d, \Psi_k^d, \zeta_k^d, \lambda_k^d, \tilde{\mathbf{C}}_k^d, \tilde{\boldsymbol{\Theta}}_k^d \mid \tilde{b} \sum_{q \in \kappa_{dm}} \gamma_{mk}^d (\tilde{c}_{mq,k}^d)^2 \leq \frac{1}{N_t}, 0 \leq \tilde{\theta}_{l,k}^d \leq 1, \right. \quad (25a)$$

$$\lambda_k^d \leq \sum_{m \in \mathcal{M}_k^d} A_{mk}^d \tilde{c}_{mk,k}^d, \sum_{m=1}^M \sum_{q \in \kappa_{dm}} B_{kmq}^d (\tilde{c}_{mq,k}^d)^2 + \sum_{l=1}^{K_u} D_{kl}^d \tilde{\theta}_{l,k}^d + 1 \leq \Lambda^{(n)} \left(\frac{(\lambda_k^d)^2}{\zeta_k^d} \right), \quad (25b)$$

$$(\Psi_k^d)^2 \leq \tau_f \log_2(1 + \zeta_k^d), P_{\text{fix}} + N_t \rho_d N_0 \sum_{m \in \mathcal{M}_k^d} \frac{1}{\alpha_m} \gamma_{mk}^d (\tilde{c}_{mk,k}^d)^2 + P_{\text{tc},k}^d \leq \Lambda^{(n)} \left(\frac{(\Psi_k^d)^2}{f_k^d} \right), \quad (25c)$$

$$\tilde{c}_{mq,k}^d \geq 0 \forall q = 1 \text{ to } K_d, \lambda_k^d \geq 0, \log_2(1 + \zeta_k^d) \geq S_{ok}^d / \tau_f \}, \quad (25d)$$

$$\mathcal{S}_l^{u,(n)} = \left\{ f_l^u, \Psi_l^u, \zeta_l^u, \lambda_l^u, \tilde{\mathbf{C}}_l^u, \tilde{\boldsymbol{\Theta}}_l^u \mid \tilde{b} \sum_{k \in \kappa_{dl}} \gamma_{lk}^d (\tilde{c}_{mk,l}^u)^2 \leq \frac{1}{N_t}, 0 \leq \tilde{\theta}_{q,l}^u \leq 1 \forall q = 1 \text{ to } K_u, \right. \quad (25e)$$

$$(\lambda_l^u)^2 \leq A_l^u \tilde{\theta}_{l,l}^u, \sum_{q=1}^{K_u} B_{lq}^u \tilde{\theta}_{q,l}^u + \sum_{i=1}^M \sum_{k \in \kappa_{di}} D_{lik}^u (\tilde{c}_{ik,l}^u)^2 + E_l^u \tilde{\theta}_{l,l}^u + F_l^u \leq \Lambda^{(n)} \left(\frac{(\lambda_l^u)^2}{\zeta_l^u} \right), \quad (25f)$$

$$(\Psi_l^u)^2 \leq \tau_f \log_2(1 + \zeta_l^u), P_{\text{fix}} + \rho_u N_0 \frac{1}{\alpha_l^u} \tilde{\theta}_{l,l}^u + P_{\text{tc},l}^u \leq \Lambda^{(n)} \left(\frac{(\Psi_l^u)^2}{f_l^u} \right), \quad (25g)$$

$$\tilde{c}_{mk,l}^u \geq 0, \log_2(1 + \zeta_l^u) \geq S_{ol}^u / \tau_f \}. \quad (25h)$$

Here $\tilde{C}_k^d, \tilde{C}_l^u \in \mathbb{C}^{M \times K_d}$ and $\tilde{\Theta}_k^d, \tilde{\Theta}_l^u \in \mathbb{C}^{K_u \times 1}$ are local copies at the D-server of the corresponding global variables at the C-server, which are denoted as $\tilde{C} \in \mathbb{C}^{M \times K_d}$ and $\tilde{\Theta} \in \mathbb{C}^{K_u \times 1}$ respectively, and represent the downlink and uplink power control coefficients, C and Θ , in **P6**. We note that each D-server has its local power control variables and hence the constraints in (25), which are all convex, are independent for each D-server. This ensures that the sets $\mathcal{S}_k^{d,(n)}$ and $\mathcal{S}_l^{u,(n)}$ are convex. We define the sets of local variables for the D-servers corresponding to the downlink and uplink UEs as $\Omega_k^d \triangleq [\tilde{C}_k^d, \tilde{\Theta}_k^d, f_k^d, \Psi_k^d, \lambda_k^d, \zeta_k^d]$ and $\Omega_l^u \triangleq [\tilde{C}_l^u, \tilde{\Theta}_l^u, f_l^u, \Psi_l^u, \lambda_l^u, \zeta_l^u]$ respectively. We now reformulate **P6** as follows

$$\begin{aligned} \mathbf{P7} : \quad & \max_{\tilde{C}, \tilde{\Theta}, \Omega_k^d, \Omega_l^u} \sum_{k=1}^{K_d} w_k^d f_k^d + \sum_{l=1}^{K_u} w_l^u f_l^u \\ \text{s.t.} \quad & \Omega_k^d \in \mathcal{S}_k^{d,(n)}, \Omega_l^u \in \mathcal{S}_l^{u,(n)}, \end{aligned} \quad (26a)$$

$$\tilde{C}_k^d = \tilde{C}, \tilde{C}_l^u = \tilde{C}, \quad (26b)$$

$$\tilde{\Theta}_k^d = \tilde{\Theta}, \tilde{\Theta}_l^u = \tilde{\Theta}. \quad (26c)$$

To ensure that the global variables at the C-server have identical local copies maintained at the D-servers, we introduce the consensus constraints (26b)-(26c). The ADMM algorithm can now be readily applied to **P7** as it is in the global consensus form [26]. We denote $\varepsilon \triangleq \{d, u\}$ to denote downlink and uplink, respectively; $\phi \triangleq \{k, l\}$ to denote k th downlink UE and l th uplink UE, respectively. The sub-problems of the individual D-servers can now be written as follows

$$\mathbf{P7b} : \max_{\tilde{C}, \tilde{\Theta}, \Omega_\phi^\varepsilon} w_\phi^\varepsilon f_\phi^\varepsilon \quad \text{s.t.} \quad \Omega_\phi^\varepsilon \in \mathcal{S}_\phi^{\varepsilon,(n)}, \tilde{C}_\phi^\varepsilon = \tilde{C}, \tilde{\Theta}_\phi^\varepsilon = \tilde{\Theta}.$$

We now define auxiliary functions for the objective in **P7b** as follows

$$q_\phi^\varepsilon(\Omega_\phi^\varepsilon) \triangleq \begin{cases} w_\phi^\varepsilon f_\phi^\varepsilon, & \Omega_\phi^\varepsilon \in \mathcal{S}_\phi^{\varepsilon,(n)}, \\ -\infty, & \text{otherwise.} \end{cases} \quad (28)$$

We write, using (28), the augmented Lagrangian function for **P7** as

$$\begin{aligned} \mathcal{L}^{(n)} & \left(\tilde{C}, \tilde{\Theta}, \{\Omega_k^d, \chi_k^d, \xi_k^d\}, \{\Omega_l^u, \chi_l^u, \xi_l^u\} \right) \\ & = \sum_{k=1}^{K_d} \left(q_k^d(\Omega_k^d) - \langle \chi_k^d, \tilde{C}_k^d - \tilde{C} \rangle - \frac{\rho_C}{2} \|\tilde{C}_k^d - \tilde{C}\|_F^2 - \langle \xi_k^d, \tilde{\Theta}_k^d - \tilde{\Theta} \rangle - \frac{\rho_\theta}{2} \|\tilde{\Theta}_k^d - \tilde{\Theta}\|^2 \right) \\ & + \sum_{l=1}^{K_u} \left(q_l^u(\Omega_l^u) - \langle \chi_l^u, \tilde{C}_l^u - \tilde{C} \rangle - \frac{\rho_C}{2} \|\tilde{C}_l^u - \tilde{C}\|_F^2 - \langle \xi_l^u, \tilde{\Theta}_l^u - \tilde{\Theta} \rangle - \frac{\rho_\theta}{2} \|\tilde{\Theta}_l^u - \tilde{\Theta}\|^2 \right), \end{aligned} \quad (29)$$

where $\rho_C, \rho_\theta > 0$ are the penalty parameters corresponding to the global variables \tilde{C} and $\tilde{\Theta}$

respectively, and $\chi_\phi^\varepsilon \in \mathbb{C}^{M \times K_d}$, $\xi_\phi^\varepsilon \in \mathbb{C}^{K_u \times 1}$ are the Lagrangian variables associated with the equality constraints (26b) and (26c), respectively. The quadratic penalty terms are added to the objective to penalise equality constraints violations, and to enable the ADMM to converge by relaxing constraints of finiteness and strict convexity [26].

We note that the augmented Lagrangian in (29) is not decomposable in general for the problem formulation in **P7b** [25]. The auxiliary functions defined in (28) enable us to decompose it and formulate sub-problems for the D-servers. In ADMM method, the D-servers independently solve the sub-problems and update the local variables, which are collected by the C-server to update the global variables [26]. In the $(p+1)$ th iteration, following steps are executed in succession.

1) *Local computation*: The D-servers for each UE solve **P8** to update the local variables as

$$\begin{aligned} \mathbf{P8} : \Omega_\phi^{\varepsilon, (p+1)} = \arg \max_{\Omega_\phi^\varepsilon} & q_\phi^\varepsilon(\Omega_\phi^\varepsilon) - \langle \chi_\phi^{\varepsilon, (p)}, \tilde{C}_\phi^\varepsilon - \tilde{C}^{(p)} \rangle - \frac{\rho_C^{(p)}}{2} \|\tilde{C}_\phi^\varepsilon - \tilde{C}^{(p)}\|_F^2 \\ & - \langle \xi_\phi^{\varepsilon, (p)}, \tilde{\Theta}_\phi^\varepsilon - \tilde{\Theta}^{(p)} \rangle - \frac{\rho_\theta^{(p)}}{2} \|\tilde{\Theta}_\phi^\varepsilon - \tilde{\Theta}^{(p)}\|^2. \end{aligned} \quad (30)$$

2) *Lagrangian multipliers update*: The D-servers now update the Lagrangian multipliers as

$$\chi_\phi^{\varepsilon, (p+1)} = \chi_\phi^{\varepsilon, (p)} + \rho_C^{(p)} (\tilde{C}_\phi^{\varepsilon, (p+1)} - \tilde{C}^{(p)}) \text{ and } \xi_\phi^{\varepsilon, (p+1)} = \xi_\phi^{\varepsilon, (p)} + \rho_\theta^{(p)} (\tilde{\Theta}_\phi^{\varepsilon, (p+1)} - \tilde{\Theta}^{(p)}). \quad (31)$$

3) *Global aggregation and computation*: The C-server now collects the updated local variables and Lagrangian multipliers from the D-servers and updates the global variables $\{\tilde{C}, \tilde{\Theta}\}$ as

$$\mathbf{P9} : \{\tilde{C}, \tilde{\Theta}\}^{(p+1)} = \arg \max_{\tilde{C}, \tilde{\Theta}} \mathcal{L}^{(n)} \left(\tilde{C}, \tilde{\Theta}, \{\Omega_k^d, \chi_k^d, \xi_k^d\}^{(p+1)}, \{\Omega_l^u, \chi_l^u, \xi_l^u\}^{(p+1)} \right).$$

Using (29) and maximizing w.r.t. each global variable, we obtain a closed form solution

$$\tilde{C}^{(p+1)} = \frac{1}{(K_u + K_d)} \left(\sum_{k=1}^{K_d} \left[\tilde{C}_k^{d, (p+1)} + \frac{1}{\rho_C^{(p)}} \chi_k^{d, (p+1)} \right] + \sum_{l=1}^{K_u} \left[\tilde{C}_l^{u, (p+1)} + \frac{1}{\rho_C^{(p)}} \chi_l^{u, (p+1)} \right] \right), \quad (32)$$

$$\tilde{\Theta}^{(p+1)} = \frac{1}{(K_u + K_d)} \left(\sum_{k=1}^{K_d} \left[\tilde{\Theta}_k^{d, (p+1)} + \frac{1}{\rho_\theta^{(p)}} \xi_k^{d, (p+1)} \right] + \sum_{l=1}^{K_u} \left[\tilde{\Theta}_l^{u, (p+1)} + \frac{1}{\rho_\theta^{(p)}} \xi_l^{u, (p+1)} \right] \right). \quad (33)$$

4) *Residue calculation and penalty parameter updates*: The C-server now calculates the squared magnitude of the primal and dual residuals, denoted as \mathbf{r}_{ADMM} and \mathbf{s}_{ADMM} respectively, as [26]

$$\|\mathbf{r}_{\text{ADMM}}^{(p+1)}\|_2^2 = \sum_{k=1}^{K_d} \left(\|\tilde{C}_k^d - \tilde{C}\|_F^2 + \|\tilde{\Theta}_k^d - \tilde{\Theta}\|_2^2 \right)^{(p+1)} + \sum_{l=1}^{K_u} \left(\|\tilde{C}_l^u - \tilde{C}\|_F^2 + \|\tilde{\Theta}_l^u - \tilde{\Theta}\|_2^2 \right)^{(p+1)}, \quad (34)$$

$$\|\mathbf{s}_{\text{ADMM}}^{(p+1)}\|_2^2 = (K_u + K_d) \left(\|\tilde{C}^{(p+1)} - \tilde{C}^{(p)}\|_F^2 + \|\tilde{\Theta}^{(p+1)} - \tilde{\Theta}^{(p)}\|_2^2 \right). \quad (35)$$

Using (34)-(35), the C-server updates penalty parameters for the $(p+1)$ th ADMM iteration as

$$\rho_{\{C,\theta\}}^{(p+1)} = \begin{cases} \rho_{\{C,\theta\}}^{(p)} \vartheta^{\text{incr}}, & \|r^{(p+1)}\|_2 > \mu \|s^{(p+1)}\|_2, \\ \rho_{\{C,\theta\}}^{(p)} / \vartheta^{\text{decr}}, & \|s^{(p+1)}\|_2 > \mu \|r^{(p+1)}\|_2, \\ \rho_{\{C,\theta\}}^{(p)}, & \text{otherwise.} \end{cases} \quad (36)$$

The parameters $\mu > 1, \vartheta^{\text{incr}} > 1, \vartheta^{\text{decr}} > 1$ are tuned to obtain good convergence [29].

Initialization for ADMM: At the $(n+1)$ th SCA iteration, we initialize the global variables at the C-server and their local copies at the D-servers with the SCA iteration variables as

$$\tilde{c}_{mk}^{(1)} = c_{mk}^{(n+1)}, \tilde{\theta}_l^{(1)} = \theta_l^{(n+1)}, \tilde{C}_k^{d,(1)} = \tilde{C}_l^{u,(1)} = \tilde{C}^{(1)}, \tilde{\Theta}_k^{d,(1)} = \tilde{\Theta}_l^{u,(1)} = \tilde{\Theta}^{(1)}. \quad (37)$$

ADMM Convergence Criterion: The ADMM can be said to have converged at iteration P if the primal residue is within a pre-determined tolerance limit ϵ_{ADMM} i.e., $\|r^{(P)}\|_2 \leq \epsilon_{\text{ADMM}}$.

The steps (30), (31), (32)-(33) and (36) are iterated until convergence, after which we obtain the locally optimal power control coefficients $\{\tilde{C}^*, \tilde{\Theta}^*\}$. We assign them to the iterates for the $(n+1)$ th SCA iteration, i.e., $C^{(n+1)} = \tilde{C}^*, \Theta^{(n+1)} = \tilde{\Theta}^*$. This concludes the n th SCA iteration.

The SCA is iterated till convergence. The steps for decentralized WSEE maximization using SCA and ADMM are summarized in Algorithm 4.

Algorithm 4: Decentralized WSEE maximization algorithm using SCA and ADMM

Input: i) Initialize power control coefficients for SCA, $\{C, \Theta\}^{(1)}$ by allocating equal power to downlink UEs and maximum power to uplink UEs. Set $n = 1$. Initialize $\{f^d, f^u, \Psi^d, \Psi^u, \zeta^d, \zeta^u, \lambda^d, \lambda^u\}^{(1)}$ by replacing inequalities (23c), (24a)-(24b), (22b) and (24c)-(24d) by equality, in turn.

Output: Globally optimal power control coefficients $\{C, \Theta\}^*$

```

1 while  $\|r_{\text{SCA}}\| \leq \epsilon_{\text{SCA}}$  do
2   Set  $p = 1$ . Initialize global variables at C-server,  $\{\tilde{C}, \tilde{\Theta}\}^{(1)}$ , and local variables at D-servers,  $\Omega_\phi^{\varepsilon,(1)}$ , using (37)
   and replacing inequalities (25b)-(25c) and (25f)-(25g) by equality.
3   while  $\|r_{\text{ADMM}}\| \leq \epsilon_{\text{ADMM}}$  do
4     Substitute  $\{C, \Theta, f^d, f^u, \Psi^d, \Psi^u, \zeta^d, \zeta^u, \lambda^d, \lambda^u\}^{(n)}$  in (25) to obtain feasible sets  $\mathcal{S}_\phi^{\varepsilon,(n)}$ .
     Solve P8 at respective D-servers to update local variables  $\Omega_\phi^{\varepsilon,(p+1)}$ .
     Solve (31) at respective D-servers to update Lagrangian multipliers  $\{\chi, \xi\}_\phi^{\varepsilon,(p+1)}$ .
     At the C-server, collect the local variables  $\{\tilde{C}, \tilde{\Theta}\}_\phi^{\varepsilon,(p+1)}$ , and the Lagrangian multipliers,  $\{\chi, \xi\}_\phi^{\varepsilon,(p+1)}$ ,
     from the D-servers and solve (32)-(33) to update the global variables  $\tilde{C}^{(p+1)}, \tilde{\Theta}^{(p+1)}$ .
     At the C-server, update penalty parameters  $\rho_{C,\theta}^{(p+1)}$  according to (36) and broadcast them to all D-servers.
5   Update  $C^{(n+1)} = \tilde{C}^*, \Theta^{(n+1)} = \tilde{\Theta}^*$  and obtain  $\{f^d, f^u, \lambda^d, \lambda^u, \Psi^d, \Psi^u, \zeta^d, \zeta^u\}^{(n+1)}$  by replacing the
   inequalities (23c), (24a)-(24b), (22b) and (24c)-(24d) by equality.
6 return  $\{C, \Theta\}^*$ .
```

Remark 3. Convergence of proposed decentralized algorithm: Algorithm 4 uses the iterative SCA technique with each SCA iteration involving the ADMM approach. The algorithm is guaranteed to converge if both SCA and ADMM converge. As discussed in Remark 2, the SCA iterative procedure surely converges to a KKT point of **P2**. For a given SCA iteration, the convergence of ADMM is guaranteed and investigated in detail in [26].

Remark 4. Feasibility of quality-of-service (QoS) constraints: The QoS constraints in (19a) and (20) may result in “congestion”, which arises when all UEs are not able to fulfill the minimum QoS requirements [30]. The optimization problem in Algorithm 4 then becomes infeasible. It is, therefore, important to have a non-empty feasible set for the algorithm to work appropriately. One possible solution is to remove the UEs that are making the problem infeasible. Determining which UEs need to be removed is, however, a difficult problem and is an area of ongoing investigation. Reference [30] recently investigated this issue for the downlink of a HD CF mMIMO system and proposed a solution for the power minimization problem. Its extension to the current FD system with both downlink and uplink, coupled FD interference terms, and for WSEE maximization is non-trivial. It is, however, an important direction for future research.

Remark 5. Implementability: The maximal ratio combiner/beamformer considered herein is the simplest receiver/transmitter for a distributed cell-free mMIMO system [3]. Further, the power optimization algorithms require only long-term fading channel coefficients, which remain constant for hundreds of coherence intervals [23]. This is in contrast to the existing work in SE-GEE maximization of FD cell-free massive MIMO systems in [14], which requires instantaneous channel. The current optimization problem whose reduced complexity is discussed below, therefore, needs to be solved over a relaxed time frame, which makes it easily implementable.

C. Computational complexity of centralized and decentralized algorithms

Before beginning this study, it is worth noting that both centralized Algorithm 3 and decentralized Algorithm 4 comprise of multiple steps that involve solving simple closed form expressions. These steps consume much lesser time than the ones which solve a GCP, typically using interior points methods [25]. We therefore compare the per-iteration complexity of centralized and decentralized algorithms by calculating the complexity of solving the respective GCPs.

- Algorithm 3 solves **P6** in step-1 of each SCA iteration, which has $4(K_u + K_d) + K_u + MK_d$ real variables and $6(K_u + K_d) + M + MK_d$ linear constraints. It has a worst-case computational complexity $\mathcal{O}\left((10(K_u + K_d) + K_u + M + 2MK_d)^{3/2}(4(K_u + K_d) + K_u + MK_d)^2\right)$ [31].

- Algorithm 4, in step-2 of each ADMM iteration, solves **P8** at the D-servers *in parallel* to update the local variables. We, therefore, need to analyse the computational complexity at *any one of the* D-servers. Since the downlink has an additional constraint (second one in (25d)), we consider a downlink D-server for worst-case complexity analysis, which in **P8** has $MK_d + K_u + 4$ real variables and $MK_d + M + K_u + 6$ linear constraints. It will have a worst-case computational complexity of $\mathcal{O}((2MK_d + M + 2K_u + 10)^{3/2} (MK_d + K_u + 4)^2)$ [31].

We consider $K_d = K_u = K/2$ uplink and downlink UEs for this analysis. We observe that for a large K , Algorithm 4 has a much lower computational complexity than Algorithm 3.

D. Overhead/cost:

We note that the *centralized* Algorithm 2 and *decentralized* Algorithm 3 require only large-scale channel coefficients, which remain constant over *hundreds* of coherence intervals [23]. In the current design, the APs estimate large-scale fading coefficients and send them to the CPU. For the FD system, we also need to measure the intra-/inter-AP and inter-UE large scale fading coefficients and communicate them to the CPU. Since APs remain largely static, the intra-/inter-AP large-scale channel fading coefficients can be estimated *just once* over a *very large* number of coherence intervals [5], [6]. The inter-UE fading coefficients are small in number and can be estimated at very low overhead. Another overhead arises when the CPU communicates the optimal power control coefficients to the APs. We now explicitly compute these overheads in the Table I below in terms of complex scalar terms required to be transmitted over the fronthaul links for each iteration of Algorithm 4. We consider an FD cell-free massive MIMO system with M APs, K_u uplink UEs and K_d downlink UEs. Further, Algorithm 4 requires only on the large-scale channel statistics, and hence needs to be executed once for *hundreds* of coherence intervals. *Therefore, for each coherence interval, these overheads are quite insignificant.*

Table I: Various overheads in decentralized WSEE maximization for a FD CF massive MIMO system

Parameter	Complex scalar terms per iteration
AP-UE channel state	$M \times (K_d + K_u)$
Inter-UE channel state	$K_d \times K_u$
Intra-/Inter-AP channel state	$M \times M$
Downlink power control coefficients	$M \times K_d$
Uplink power control coefficients	K_u

V. SIMULATION RESULTS

We now numerically investigate the SE and WSEE of a FD CF mMIMO system with limited-capacity fronthaul links. We assume a realistic system model wherein the M APs, K_d downlink

UEs and K_u uplink UEs are all scattered randomly in a square of size $D \text{ km} \times D \text{ km}$. To avoid the boundary effects [2], we wrap the APs and UEs around the edges [5]. We denote $\varepsilon \triangleq \{d, u\}$ to denote downlink and uplink, respectively; $\phi \triangleq \{k, l\}$ to denote k th downlink UE and l th uplink UE, respectively. The large-scale fading coefficients, $\beta_{m\phi}^\varepsilon$, are modeled as [11]

$$\beta_{m\phi}^\varepsilon = 10^{\frac{\text{PL}_{m\phi}^\varepsilon}{10}} 10^{\frac{\sigma_{\text{sd}} z_{m\phi}^\varepsilon}{10}}. \quad (38)$$

Here $10^{\frac{\sigma_{\text{sd}} z_{m\phi}^\varepsilon}{10}}$ is the log-normal shadowing factor with a standard deviation σ_{sd} (in dB) and $z_{m\phi}^\varepsilon$ follows a two-components correlated model [2] as $z_{km} = \sqrt{\delta} a_m + \sqrt{1-\delta} b_k$ with $a_m \sim \mathcal{CN}(0, 1)$, $\mathbb{E}\{a_m, a'_m\} = 2^{-\frac{d_{\text{AP}}(m, m')}{d_{\text{decorr}}}}$, $b_k \sim \mathcal{CN}(0, 1)$, $\mathbb{E}\{b_k, b'_k\} = 2^{-\frac{d_{\text{UE}}(k, k')}{d_{\text{decorr}}}}$ being independent random variables. The terms $d_{\text{AP}}(m, m')$ and $d_{\text{UE}}(k, k')$ denote Euclidean distances between the m th and m' th APs and the k th and k' th UEs, respectively. The term d_{decorr} is the decorrelation distance, typically of the order $20A^\circ - 200m$ [2] ($1A^\circ = 10^{-10} \text{ m}$), and $0 \leq \delta \leq 1$ determines correlation at APs and UEs. The path loss $\text{PL}_{m\phi}^\varepsilon$ (in dB) follows a three-slope model [2], [5].

$$\text{PL}_{mk}^d = \begin{cases} -35 \log(d_{mk}) - Z, & d_{mk} > d_{ub} \\ -20 \log(d_{mk}) - 15 \log(d_{ub}) - Z, & d_{lb} < d_{mk} < d_{ub} \\ -20 \log(d_{lb}) - 15 \log(d_{ub}) - Z, & d_{mk} < d_{lb}. \end{cases} \quad (39)$$

The factor Z , similar to [2], is defined as $Z = 45.5 + 35.46 \log(f_0) - h_0(1.11 \log_{10}(f_0) - 0.7) - 13.82 \log(h_1)$. Here, f_0 is the carrier frequency (in MHz) and h_0, h_1 denote the UE and AP antenna heights, respectively (in m). We, similar to [5], model the large-scale fading coefficients for the inter-AP RI channels, i.e., $\beta_{\text{RI}, mi}$, $\forall i \neq m$, as in (38), and assume that the large-scale fading for the intra-AP RI channels, which experience no shadowing, are modeled as $\beta_{\text{RI}, mm} = 10^{\frac{\text{PL}_{\text{RI}}(\text{dB})}{10}}$. The inter-UE large scale fading coefficients, $\tilde{\beta}_{kl}$, are also modeled similar to (38). We consider, for brevity, same number of quantization bits, ν , and same capacity, C_{fb} , on all fronthaul links. We, henceforth, denote the transmit powers on the downlink and uplink as $p_d (= \rho_d N_0)$ and $p_u (= \rho_u N_0)$, respectively, and the pilot transmit power as $p_t (= \rho_t N_0)$. Similar to [2], [5], [8], [11], [12], we fix the values for the system model and power consumption model parameters, unless mentioned otherwise, as given in Table II.

Validation of SE expressions: We consider an FD CF mMIMO system with i) $M = \{16, 32\}$ APs, each having $N_t = N_r = 8$ transmit and receive antennas, $K_d = 12$ downlink UEs and $K_u = 8$ uplink UEs; and ii) unequal uplink and downlink transmit power i.e., $p_d = 2p_u = p$. We verify in Fig. 2a the tightness of the SE lower bound derived in (14)-(15), labeled as LB, by comparing

Table II: Full-Duplex Cell-Free mMIMO system model and power consumption model parameters

Parameter	Value	Parameter	Value
$D, d_{ub}, d_{lb}, d_{\text{decorr}}$ (in m)	1000, 50, 10, 100	h_0, h_1 (in m)	1.65, 15
Shadowing parameters $\sigma_{\text{sd}}, \delta$	2 dB, 0.5	τ_c, T_c	200, 1 ms
Carrier frequency, f_0	1.9 GHz	Bandwidth, B	20 Mhz
Fronthaul parameters ν, C_{fh}	2, 10 Mbps	$\gamma_{\text{RI}}, \text{PL}_{\text{RI}}$ (in dB)	-20, -81.1846
$P_{\text{ft}}, P_{0,m}, P_{c,m} = P_{\text{tc},k}^d = P_{\text{tc},l}^u, p_t$ (in W)	10, 0.825, 0.2, 0.2	N_0, α_m, α'_l	-121.4 dB, 0.39, 0.3

it with the numerically-obtained ergodic SE in (10), labeled as upper-bound (UB) as it requires instantaneous CSI. The large-scale fading coefficients are set according to a practical FD CF channel model with parameters specified in Table II. We, similar to [2], [11], allocate equal power to all downlink UEs and full power to all uplink UEs, i.e., $\eta_{mk} = (bN_t (\sum_{k \in \kappa_{dm}} \gamma_{mk}^d))^{-1}, \forall k \in \kappa_{dm}$ and $\theta_l = 1$. We see that the derived lower bound is tight for both values of M .

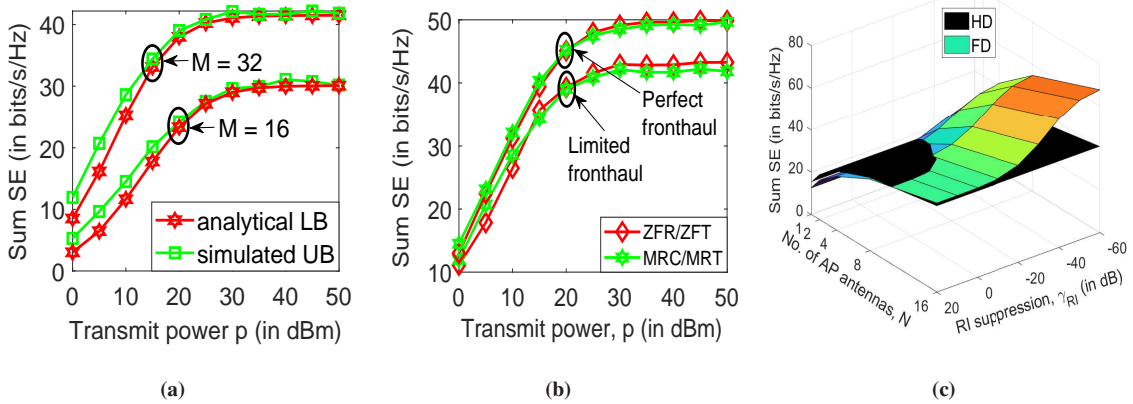


Fig. 2: a) Sum SE vs transmit power, with $N_t = N_r = 8, K_d = 12, K_u = 8$; b) Sum SE of MR and ZF transceivers with $M = 32, N_t = N_r = 8, K_d = 12, K_u = 8$; and c) Sum SE vs RI suppression levels, with $M = 32, K_d = 12, K_u = 8$.

We now fix $M = 32$ and compare in Fig. 2b the sum SE of MRC/MRT and zero forcing reception/zero forcing transmission (ZFR/ZFT) transceivers when applied to FD CF systems [32]. We consider two fronthaul cases: i) perfect high-capacity with $\tilde{a} = \tilde{b} = 1$, and ii) limited $C_{\text{fh}} = 10$ Mbps capacity with $\nu = 2$ quantization bits. We see that for both fronthauls, the MRC/MRT transceiver for the scenario considered herein, although slightly inferior at high transmit power, performs reasonably well when compared with computationally-intensive ZFR/ZFT transceiver. With limited fronthaul, the sum SE significantly drops, as quantization attenuates and distorts the signal and limits the number of UEs that each AP can serve (see (9)).

Sum SE - FD and HD comparison: We consider an FD CF mMIMO system with $M = 32$ APs, $K_d = 12$ downlink UEs, $K_u = 8$ uplink UEs and with transmit powers $p_d = 30$ dBm,

$p_u = 27$ dBm on the downlink and uplink. We compare in Fig. 2c the FD CF mMIMO system with varying levels of RI suppression factor γ_{RI} and an equivalent HD system which serves uplink and downlink UEs in time-division duplex mode. For the HD system, we i) set $\gamma_{\text{RI}} = 0$ and inter-UE channel gains $\tilde{\beta}_{kl} = 0$; ii) use all AP antennas, i.e., $N = (N_t + N_r)$, during uplink and downlink transmission; and iii) multiply sum SE with a factor of $(1/2)$. We see that the FD system has a significantly higher sum SE than an equivalent HD system, provided the RI suppression is good ($\gamma_{\text{RI}} \leq -10$ dB). The sum SE does not double, even with significant RI suppression $\gamma_{\text{RI}} \leq -40$ dB. This is due to the UDI experienced by the downlink UEs in a FD CF mMIMO system as shown in Fig. 1, which cannot be mitigated by RI suppression at the APs.

WSEE metric - influence of weights: We now demonstrate that the WSEE metric can accommodate the heterogeneous EE requirements of both uplink and downlink UEs. For this study, we consider a particular realization of a FD CF mMIMO system with a transmit power $p_d = 2p_u = 30$ dBm, $M = 32$ APs, $K_d = K_u = K/2 = 2$ uplink and downlink UEs and $N_t = N_r = N = 2$ transmit and receive antennas on each AP, with QoS constraints $S_{ok} = S_{ol} = 0.1$ bits/s/Hz. We plot the individual EEs of the uplink (UL) and downlink (DL) UEs versus the SCA iteration index for centralized WSEE maximization, using Algorithm 3, for two different combinations of UE weights. Weights w_1 and w_2 are associated with DL UE 1 and DL UE 2, while weights w_3 and w_4 are associated with UL UE 1 and UL UE 2, respectively.

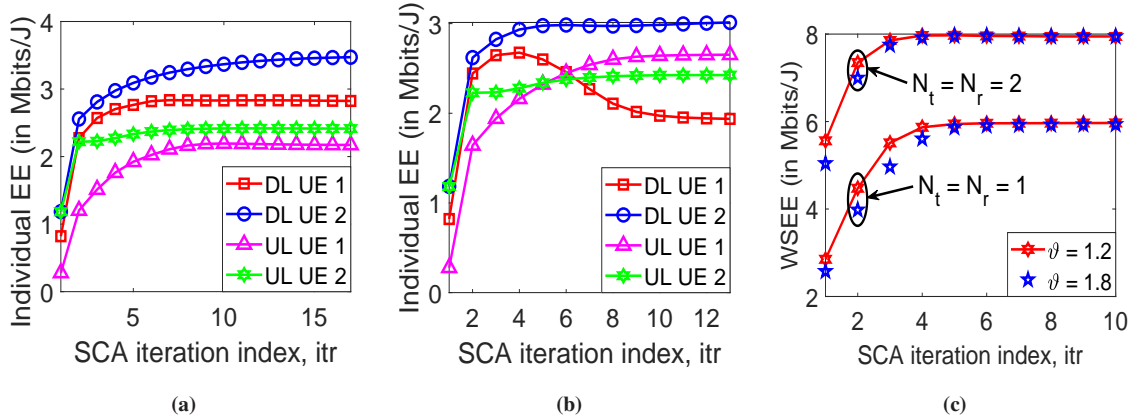


Fig. 3: Effect of UE priorities on individual EEs with $M = 32$, $K_d = K_u = 2$, $N_t = N_r = 2$ and $S_{ok} = S_{ol} = 0.1$ bits/s/Hz: (a) $w_1 = w_2 = w_3 = w_4 = 0.25$, (b) $w_1 = 0.08, w_2 = 0.02, w_3 = 0.5, w_4 = 0.4$; c) Convergence of decentralized algorithm.

We plot in Fig. 3a and Fig. 3b the individual EEs of UL and DL UEs, with: i) equal weights ($w_1 = w_2 = w_3 = w_4 = 0.25$), and ii) $w_1 = 0.08, w_2 = 0.02, w_3 = 0.5, w_4 = 0.4$, respectively.

In Fig. 3a, with equal weights, UEs attain an EE depending on their relative channel conditions, which clearly indicates that in terms of channel conditions, DL UE 2 \gg DL UE 1 > UL UE 2 > UL UE 1. In Fig. 3b, the weights are chosen in an order which is opposite to the channel conditions. The EEs of the UL UEs dominate the EE of DL UE 1, while reversing their relative order. DL UE 2, with excellent channel, still attains a high EE, although lower than in Fig. 3a.

Convergence of decentralized ADMM algorithm: We plot in Fig. 3c the WSEE obtained using decentralized Algorithm 4 with SCA iteration index. We consider $M = 10$ APs, $K_u = K_d = K/2 = 2$ uplink and downlink UEs and $N_t = N_r = \{1, 2\}$ transmit and receive antennas on each AP at transmit power $p_d = 2p_u = p = 30$ dBm. We assume the following: i) penalty parameters $\rho_C = \rho_\theta = 0.1$; ii) penalty parameter update threshold factor $\mu = 10$; iii) ADMM convergence threshold $\epsilon_{\text{ADMM}} = 0.01$; and iv) SCA convergence threshold $\epsilon_{\text{SCA}} = 0.001$. We consider two values of the penalty update parameter: $\vartheta = \{1.2, 1.8\}$. We note that the algorithm in both cases converges marginally quicker with $\vartheta = 1.2$. A smaller penalty update parameter is therefore beneficial as then changes in the penalty parameters are not too abrupt, and a bad ADMM iteration which causes the primal and dual residues to diverge is, consequently, not overly responded to [29]. We therefore fix $\vartheta = 1.2$ for the rest of the simulations.

WSEE variation with parameters: We now vary WSEE with important system parameters and obtain crucial insights into energy-efficient FD CF mMIMO system designing. We consider $M = 32$ APs, $N_t = N_r = N = 8$ AP transmit and receive antennas, $K_d = 12$ downlink UEs, $K_u = 8$ uplink UEs and QoS constraints $S_{ok} = S_{ol} = 0.1$ bits/s/Hz, unless mentioned otherwise.

We plot in Fig. 4a the WSEE by simultaneously varying downlink and uplink transmit power as $p_d = 2p_u = p$. We consider centralized and decentralized optimal power allocation (OPA) approaches from Algorithm 3 and Algorithm 4, respectively. We compare them with three sub-optimal power allocation schemes: i) equal power allocation of type 1, labeled as “EPA 1”, where $\eta_{mk} = (bN_t (\sum_{k \in \kappa_{dm}} \gamma_{mk}^d))^{-1}, \forall k \in \kappa_{dm}$ and $\theta_l = 1$ [11], [12], ii) equal power allocation of type 2, labeled as “EPA 2”, where $\eta_{mk} = (bN_t K_{dm} \gamma_{mk}^d)^{-1}, \forall k \in \kappa_{dm}$ and $\theta_l = 1$ [11], and iii) random power allocation, labeled as “RPA”, where power control coefficients are chosen randomly from a uniform distribution between 0 and the “EPA 1” value. We note that i) the existing literature has not yet optimized the WSEE metric for CF mMIMO systems, and hence we can only compare with above sub-optimal schemes; ii) the decentralized ADMM approach, with lower computational complexity, has same WSEE as the centralized one; and iii) both

decentralized and centralized approaches far outperform the baseline schemes.

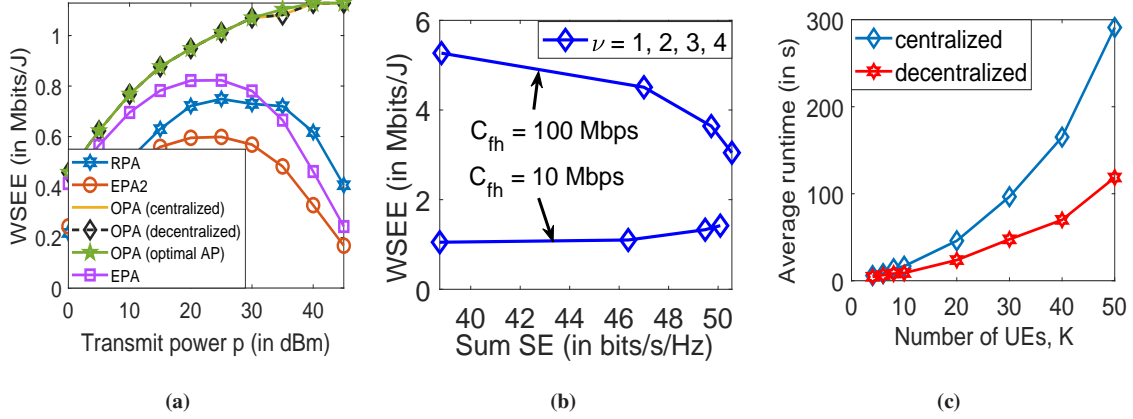


Fig. 4: WSEE vs (a) Maximum transmit power and (b) Sum SE by varying $\nu = 1$ to 4, with $M = 32$, $K_d = K_u = 10$, $N_t = N_r = 2$ and $S_{oh} = S_{ot} = 0.1$ bits/s/Hz; c) Comparison of per-iteration runtime for decentralized and centralized algorithms.

Comparison between fair and optimal AP selection: We now compare in Fig. 4a the proposed fair AP selection Algorithm 1 with the optimal AP selection in [33] (labelled as OPA (optimal AP)) after suitable modifications. These modification are required because it i) is proposed for the *downlink CF mMIMO system with perfect fronthaul links*; and ii) minimizes power instead of maximizing WSEE. We observe from Fig. 4a that the proposed fair AP selection approach has similar WSEE as that of OPA (optimal AP). This is because the proposed procedure eliminates the AP-UE links that do not have sufficient channel gain and thus contribute little to the system throughput while consuming a significant amount of power. Turning off APs according to the optimal AP procedure, thus, only marginally improves the performance.

We next characterize in Fig. 4b the joint variation of WSEE and sum SE with the number of quantization bits ν in the fronthaul links. The WSEE is obtained using decentralized Algorithm 4. We consider transmit power $p_d = 2p_u = p = 30$ dBm and take two different cases: i) high fronthaul capacity, $C_{fh} = 100$ Mbps, which is sufficiently high to support all the UEs, and ii) limited fronthaul capacity, $C_{fh} = 10$ Mbps, which limits the number of UEs a single AP can serve. We observe that for $C_{fh} = 100$ Mbps, the WSEE falls with increase in ν , even though the corresponding sum SE increases. For $C_{fh} = 10$ Mbps, both sum SE and WSEE simultaneously increase with increase in ν . We explain this behavior by noting that increasing ν reduces the quantization distortion and attenuation, thereby improving the sum SE. We observe that reducing the fronthaul capacity from $C_{fh} = 100$ Mbps to $C_{fh} = 10$ Mbps reduces the sum SE slightly, as the procedure outlined in Section II-2 *fairly* retains the AP-UE links with the highest channel gains

and helps maintain the sum SE. For $C_{fh} = 100$ Mbps, the APs serve all the UEs, i.e., $K_{dm} = K_d$ and $K_{um} = K_u$, so increasing ν linearly increases the fronthaul data rate, R_{fh} (see (7)). This, as seen from (17), increases the traffic-dependent fronthaul power consumption. Using lower number (1-2) of quantization bits is therefore more energy-efficient, as it provides sufficiently good SE with a low energy consumption. However, for $C_{fh} = 10$ Mbps, K_{um} and K_{dm} have an upper limit, given by (9), which is inversely related to ν . The product, $\nu(K_{um} + K_{dm})$, remains nearly constant for all values of ν . Thus, R_{fh} (see (7)) doesn't increase with increase in ν and remains close to the capacity, C_{fh} . The traffic-dependent fronthaul power consumption, given in (17), hence, remains close to P_{ft} . A higher number (3-4) of quantization bits therefore provides a higher sum SE and hence, also maximizes the WSEE.

Latency: The *per-iteration* complexity of the *decentralized* Algorithm 4, as observed earlier in Section IV-C, is lower than the *centralized* Algorithm 3. We now demonstrate the same by comparing their *per-iteration* runtime. For this simulation, as shown in Fig. 4c, we consider an FD CF mMIMO system with $M = 32$ APs, each having $N_t = N_r = 8$ transmit and receive antennas, and plot the average runtime of each iteration by varying the total number of UEs, K , with $K_d = K_u = K/2$. We note that the decentralized algorithm has significantly lower per-iteration runtime, particularly for large UEs. Both these algorithms require only large-scale channel coefficients and hence need to be executed only once in *hundreds* of coherence intervals.

VI. CONCLUSION

We derived SE lower bound for a FD CF mMIMO wireless system with optimal uniform fronthaul quantization. Using a *two-layered* approach, we optimized WSEE using SCA framework which in each iteration solves a GCP either centrally or decentrally using ADMM. We showed how WSEE incorporates EE requirements of different UEs. We analytically and numerically demonstrated the convergence of decentralized algorithm. We showed that it achieves the same WSEE as the centralized approach with a much reduced computational complexity.

APPENDIX A

We use the optimal uniform quantization model from [8], [12]. Using Bussgang decomposition [34], the quantization function $\mathcal{Q}(x) = \tilde{a}x + \sqrt{p_x}\tilde{\zeta}_d$, where $p_x = \mathbb{E}\{|x|^2\}$ is the power of the unquantized signal x , $\tilde{a} = \frac{1}{p_x} \int_{\mathcal{X}} xh(x)f_X(x)dx$, $\tilde{b} = \frac{1}{p_x} \int_{\mathcal{X}} h^2(x)f_X(x)dx$ and $\tilde{\zeta}_d$ is the normalized distortion whose power is given as $\mathbb{E}\{\tilde{\zeta}_d^2\} = \tilde{b} - \tilde{a}^2$. Here $h(x)$ is the mid-rise uniform quantizer with $L = 2^\nu$ quantization levels rising in steps of size $\tilde{\Delta}$ and ν is the number of quantization bits. The signal-to-distortion ratio $\text{SDR} = \frac{\mathbb{E}\{(\tilde{a}x)^2\}}{p_x\mathbb{E}\{\tilde{\zeta}_d^2\}} = \frac{\tilde{a}^2}{\tilde{b} - \tilde{a}^2}$. The optimal step-size $\tilde{\Delta}_{\text{opt}}$ maximizes the SDR. The optimal \tilde{a} and \tilde{b} , are calculated using SDR, and given in Table III [8].

Table III: Optimal Uniform Quantization Parameters

ν	$\tilde{\Delta}_{\text{opt}}$	$\mathbb{E}\{\tilde{\zeta}_d^2\} = \tilde{b} - \tilde{a}^2$	\tilde{a}	ν	$\tilde{\Delta}_{\text{opt}}$	$\mathbb{E}\{\tilde{\zeta}_d^2\} = \tilde{b} - \tilde{a}^2$	\tilde{a}
1	1.596	0.2313	0.6366	4	0.3352	0.011409	0.98845
2	0.9957	0.10472	0.88115	5	0.1881	0.003482	0.996505
3	0.586	0.036037	0.96256	6	0.1041	0.0010389	0.99896

REFERENCES

- [1] T. Marzetta, “Noncooperative cellular wireless with unlimited numbers of base station antennas,” *IEEE Trans. Wireless Commun.*, vol. 9, no. 11, pp. 3590–3600, Nov. 2010.
- [2] H. Q. Ngo, A. Ashikhmin, H. Yang, E. G. Larsson, and T. L. Marzetta, “Cell-free massive MIMO versus small cells,” *IEEE Trans. Wireless Commun.*, vol. 16, no. 3, pp. 1834 – 1850, Mar. 2017.
- [3] Özlem Tugfe Demir, E. Björnson, and L. Sanguinetti, “Foundations of user-centric cell-free massive MIMO,” *Foundations and Trends® in Signal Processing*, vol. 14, no. 3-4, pp. –, 2020. [Online]. Available: <http://dx.doi.org/10.1561/20000000109>
- [4] T. Riihonen, S. Werner, and R. Wichman, “Mitigation of loopback self-interference in full-duplex MIMO relays,” *IEEE Trans. Signal Process.*, vol. 59, no. 12, pp. 5983–5993, 2011.
- [5] T. T. Vu, D. T. Ngo, H. Q. Ngo, and T. Le-Ngoc, “Full duplex cell-free massive MIMO,” in *2019 IEEE Int. Conf. on Commun.(ICC’19)*, 2019.
- [6] D. Wang, M. Wang, P. Zhu, J. Li, J. Wang, and X. You, “Performance of network-assisted full-duplex for cell-free massive MIMO,” *IEEE Trans. Commun.*, vol. 68, no. 3, pp. 1464–1478, 2020.
- [7] H. V. Nguyen, V. Nguyen, O. A. Dobre, S. K. Sharma, S. Chatzinotas, B. Ottersten, and O. Shin, “A novel heap-based pilot assignment for full duplex cell-free massive MIMO with zero-forcing,” in *2020 IEEE Int. Conf. on Commun.(ICC’20)*, 2020, pp. 1–6.
- [8] M. Bashar, K. Cumanan, A. G. Burr, H. Q. Ngo, M. Debbah, and P. Xiao, “Max–min rate of cell-free massive MIMO uplink with optimal uniform quantization,” *IEEE Trans. Commun.*, vol. 67, no. 10, pp. 6796 – 6815, Oct. 2019.
- [9] G. Femenias and F. Riera-Palou, “Cell-free millimeter-wave massive MIMO systems with limited fronthaul capacity,” *IEEE Access*, vol. 7, pp. 44 596 – 44 612, Apr. 2019.
- [10] H. Masoumi and M. J. Emadi, “Performance analysis of cell-free massive MIMO system with limited fronthaul capacity and hardware impairments,” *IEEE Trans. Wireless Commun.*, vol. 19, no. 2, pp. 1038–1053, 2020.
- [11] H. Ngo, L. Tran, T. Q. Duong, M. Matthaiou, and E. G. Larsson, “On the total energy efficiency of cell-free massive MIMO,” *IEEE Trans. on Green Commun. and Networking*, vol. 2, no. 1, pp. 25 – 39, Mar. 2018.
- [12] M. Bashar, K. Cumanan, A. G. Burr, H. Q. Ngo, E. G. Larsson, and P. Xiao, “Energy efficiency of the cell-free massive MIMO uplink with optimal uniform quantization,” *IEEE Trans. on Green Commun. and Networking*, vol. 3, no. 4, pp. 971–987, 2019.
- [13] M. Alonzo, S. Buzzi, A. Zappone, and C. D’Elia, “Energy-efficient power control in cell-free and user-centric massive MIMO at millimeter wave,” *IEEE Trans. on Green Commun. and Networking*, pp. 651 – 663, Sept. 2019.
- [14] H. V. Nguyen, V. D. Nguyen, O. A. Dobre, S. K. Sharma, S. Chatzinotas, B. Ottersten, and O. S. Shin, “On the spectral and energy efficiencies of full-duplex cell-free massive MIMO,” *IEEE J. Sel. Areas Commun.*, vol. 38, no. 8, pp. 1698–1718, 2020.

- [15] A. Zappone and E. Jorswieck, *Energy Efficiency in Wireless Networks via Fractional Programming Theory*. Hanover, MA, USA: Now Publishers Inc., Jun. 2015, vol. 11, no. 3–4. [Online]. Available: <https://doi.org/10.1561/01000000088>
- [16] C. N. Efrem and A. D. Panagopoulos, “A framework for weighted-sum energy efficiency maximization in wireless networks,” *IEEE Wireless Commun. Lett.*, vol. 8, no. 1, pp. 153–156, 2019.
- [17] E. Sharma, D. N. Amudala, and R. Budhiraja, “Energy efficiency optimization of massive MIMO FD relay with quadratic transform,” *IEEE Trans. Wireless Commun.*, vol. 19, no. 2, pp. 1429–1448, 2020.
- [18] C. Jeon, K. Li, J. R. Cavallaro, and C. Studer, “Decentralized equalization with feedforward architectures for massive MU-MIMO,” *IEEE Trans. Signal Process.*, vol. 67, no. 17, pp. 4418–4432, 2019.
- [19] J. Rodríguez Sánchez, F. Rusek, O. Edfors, M. Sarajlić, and L. Liu, “Decentralized massive MIMO processing exploring daisy-chain architecture and recursive algorithms,” *IEEE Trans. Signal Process.*, vol. 68, pp. 687–700, 2020.
- [20] Z. Zhou, J. Feng, Z. Chang, and X. Shen, “Energy-efficient edge computing service provisioning for vehicular networks: A consensus ADMM approach,” *IEEE Trans. Veh. Technol.*, vol. 68, no. 5, pp. 5087 – 5099, May 2019.
- [21] E. Sharma, S. S. Chauhan, and R. Budhiraja, “Decentralized WSEE optimization for massive MIMO two-way half-duplex AF relaying,” *IEEE Wireless Commun. Lett.*, vol. 19, no. 2, pp. 1397 – 1414, Feb. 2020.
- [22] S. Datta *et al.*, “Technical report: Full-duplex cell-free mMIMO systems: Analysis and decentralized optimization.” [Online]. Available: <https://home.iitk.ac.in/~rohitbr/pdf/technical-report-fd-cf.pdf>
- [23] A. Goldsmith, *Wireless Communications*. Cambridge University Press, NY, USA, 2005.
- [24] E. Björnson, J. Hoydis, and L. Sanguinetti, “Massive MIMO networks: Spectral, energy, and hardware efficiency,” *Foundations and Trends® in Signal Processing*, vol. 11, no. 3-4, pp. 154–655, 2017.
- [25] S. Boyd and L. Vandenberghe, *Convex optimization*. Cambridge University Press, 2004.
- [26] S. Boyd, N. Parikh, E. Chu, B. Peleato, and J. Eckstein, “Distributed optimization and statistical learning via the alternating direction method of multipliers,” *Foundations and Trends in Machine Learning*, vol. 3, no. 1, pp. 1 – 122, 2010.
- [27] G. P. W. Barry R. Marks, “Technical note - a general inner approximation algorithm for nonconvex mathematical programs,” *Operations Research*, vol. 26, no. 4, pp. 681–683, 1978.
- [28] T. Van Chien, E. Björnson, and E. G. Larsson, “Joint pilot design and uplink power allocation in multi-cell massive MIMO systems,” *IEEE Trans. Wireless Commun.*, vol. 17, no. 3, pp. 2000–2015, 2018.
- [29] B. He, H. Yang, and S. Wang, “Alternating direction method with selfadaptive penalty parameters for monotone variational inequalities,” *Journal of Optimization Theory and Applications*, vol. 106, no. 2, p. 337–356, Aug. 2000.
- [30] T. Van Chien, E. Björnson, and H. Q. Ngo, “Uplink power control in cellular massive MIMO systems: Coping with the congestion issue,” in *2020 IEEE Int. Conf. on Commun.(ICC’19) Workshops*, 2020, pp. 1–6.
- [31] A. Ben-Tal and A. Nemirovski, *Lectures on Modern Convex Optimization: Analysis, Algorithms, and Engineering Applications*. Society for Industrial and Applied Mathematics, Philadelphia, USA, 2001.
- [32] T. Van Chien, E. Björnson, and E. G. Larsson, “Joint power allocation and user association optimization for massive MIMO systems,” *IEEE Trans. Wireless Commun.*, vol. 15, no. 9, pp. 6384–6399, 2016.
- [33] —, “Joint power allocation and load balancing optimization for energy-efficient cell-free massive MIMO networks,” *IEEE Trans. Wireless Commun.*, vol. 19, no. 10, pp. 6798–6812, 2020.
- [34] P. Zillmann, “Relationship between two distortion measures for memoryless nonlinear systems,” *IEEE Signal Processing Letters*, vol. 17, no. 11, pp. 917–920, 2010.

Full-Duplex Cell-Free mMIMO Systems: Analysis and Decentralized Optimization

Soumyadeep Datta, Ekant Sharma, D.N. Amudala, Rohit Budhiraja and Shivendra S. Panwar, *Fellow*, IEEE

PROOF OF THEOREM 1

We now derive the achievable SE expression for the l th uplink UE in (15). We know from Section II that $\mathbf{g}_{ml}^u = \hat{\mathbf{g}}_{ml}^u + \mathbf{e}_{ml}^u$, where $\hat{\mathbf{g}}_{ml}^u$ and \mathbf{e}_{ml}^u are independent and $\mathbb{E}\{\|\hat{\mathbf{g}}_{ml}^u\|^2\} = N_r \gamma_{ml}^u$. We can express the desired signal for the l th uplink UE as

$$\begin{aligned} \mathbb{E}\{|\text{DS}_l^u|^2\} &= \mathbb{E}\left\{\left|\tilde{a} \sum_{m \in \mathcal{M}_l^u} \sqrt{\rho_u} \mathbb{E}\{\sqrt{\theta_l} (\hat{\mathbf{g}}_{ml}^u)^H (\hat{\mathbf{g}}_{ml}^u + \mathbf{e}_{ml}^u) s_l^u\}\right|^2\right\} \\ &= \tilde{a}^2 N_r^2 \rho_u \theta_l \left(\sum_{m \in \mathcal{M}_l^u} \gamma_{ml}^u\right)^2. \end{aligned} \quad (\text{A1})$$

We express the beamforming uncertainty for the l th uplink UE as

$$\begin{aligned} \mathbb{E}\{|\text{BU}_l^u|^2\} &= \tilde{a}^2 \rho_u \sum_{m \in \mathcal{M}_l^u} \mathbb{E}\{\|(\sqrt{\theta_l} (\hat{\mathbf{g}}_{ml}^u)^H \mathbf{g}_{ml}^u s_l^u - \mathbb{E}\{\sqrt{\theta_l} (\hat{\mathbf{g}}_{ml}^u)^H \mathbf{g}_{ml}^u s_l^u\})\|^2\} \\ &\stackrel{(a)}{=} \tilde{a}^2 \rho_u \sum_{m \in \mathcal{M}_l^u} (\mathbb{E}\{\|\hat{\mathbf{g}}_{ml}^u\|^4\} + \mathbb{E}\{|\hat{\mathbf{g}}_{ml}^u)^H \mathbf{e}_{ml}^u|^2\} - N_r^2 (\gamma_{ml}^u)^2) \theta_l \\ &\stackrel{(b)}{=} \tilde{a}^2 \rho_u \sum_{m \in \mathcal{M}_l^u} (N_r(N_r+1)(\gamma_{ml}^u)^2 + N_r \gamma_{ml}^u (\beta_{ml}^u - \gamma_{ml}^u) - N_r^2 (\gamma_{ml}^u)^2) \theta_l \\ &= \tilde{a}^2 \rho_u N_r \sum_{m \in \mathcal{M}_l^u} \gamma_{ml}^u \beta_{ml}^u \theta_l. \end{aligned} \quad (\text{A2})$$

Equality (a) is obtained by i) using $\mathbb{E}\{|s_l^u|^2\} = 1$; ii) substituting $\mathbf{g}_{ml}^u = \hat{\mathbf{g}}_{ml}^u + \mathbf{e}_{ml}^u$; iii) using the fact that \mathbf{e}_{ml}^u and $\hat{\mathbf{g}}_{ml}^u$ are zero-mean and uncorrelated; and iv) using $\mathbb{E}\{|\hat{\mathbf{g}}_{ml}^u|^2\} = N_r \gamma_{ml}^u$. Equality (b) is obtained using the results $\mathbb{E}\{\|\hat{\mathbf{g}}_{ml}^u\|^4\} = N_r(N_r+1)(\gamma_{ml}^u)^2$ [5] and $\mathbb{E}\{\|\mathbf{e}_{ml}^u\|^2\} = (\beta_{ml}^u - \gamma_{ml}^u)$.

We simplify the multi-UE interference for the l th uplink UE as

$$\begin{aligned} \mathbb{E}\{|\text{MUI}_l^u|^2\} &= \tilde{a}^2 \rho_u \sum_{m \in \mathcal{M}_l^u} \sum_{q=1, q \neq l}^{K_u} \mathbb{E}\{|\sqrt{\theta_q} (\hat{\mathbf{g}}_{ml}^u)^H \mathbf{g}_{mq}^u s_q^u - \mathbb{E}\{\sqrt{\theta_q} (\hat{\mathbf{g}}_{ml}^u)^H \mathbf{g}_{mq}^u s_q^u\}|^2\} \\ &= \tilde{a}^2 \rho_u \sum_{m \in \mathcal{M}_l^u} \sum_{q=1, q \neq l}^{K_u} \mathbb{E}\{|\hat{\mathbf{g}}_{ml}^u)^H \mathbf{g}_{mq}^u|^2\} - (\mathbb{E}\{|\hat{\mathbf{g}}_{ml}^u)^H \mathbf{g}_{mq}^u\})^2 \theta_q \stackrel{(a)}{=} \tilde{a}^2 \rho_u N_r \sum_{m \in \mathcal{M}_l^u} \sum_{q=1, q \neq l}^{K_u} \gamma_{ml}^u \beta_{mq}^u \theta_q. \end{aligned} \quad (\text{A3})$$

Equality (a) is obtained by using these facts: i) $\hat{\mathbf{g}}_{ml}^u, \mathbf{g}_{mq}^u$ are mutually independent; and

$$\text{ii) } \mathbb{E}\{|\hat{\mathbf{g}}_{ml}^u)^H \mathbf{g}_{mq}^u|^2\} = \mathbb{E}\{(\mathbf{g}_{mq}^u)^H \mathbb{E}\{(\hat{\mathbf{g}}_{ml}^u)(\hat{\mathbf{g}}_{ml}^u)^H\} \mathbf{g}_{mq}^u\} = \gamma_{ml}^u \mathbb{E}\{(\mathbf{g}_{mq}^u)^H \mathbf{g}_{mq}^u\} = N_r \gamma_{ml}^u \beta_{mq}^u.$$

We now simplify $\mathbb{E}\{|\mathbf{R}\mathbf{I}_l^u|^2\} = \tilde{a}^2 \rho_d \sum_{m \in \mathcal{M}_l^u} \sum_{i=1}^M \sum_{k \in \kappa_{di}} \mathbb{E}\{ |(\hat{\mathbf{g}}_{ml}^u)^H \mathbf{H}_{mi} (\hat{\mathbf{g}}_{ik}^d)^*|^2 \} (\tilde{a}^2 + b - \tilde{a}^2) \eta_{ik}$

$$\stackrel{(a)}{=} \tilde{a}^2 \tilde{b} N_r N_t \rho_d \sum_{m \in \mathcal{M}_l^u} \sum_{i=1}^M \sum_{k \in \kappa_{di}} \gamma_{ml}^u \gamma_{ik}^d \beta_{\text{RI},mi} \gamma_{\text{RI}} \eta_{ik}. \quad (\text{A4})$$

Equality (a) is because: i) channels $\hat{\mathbf{g}}_{ml}^u$, \mathbf{H}_{mi} and $\hat{\mathbf{g}}_{mk}^d$ are mutually independent; ii) $\gamma_{\text{RI},mi} = \beta_{\text{RI},mi} \gamma_{\text{RI}}$, $i = 1$ to M ; and iii) the result

$$\begin{aligned} \mathbb{E}\{ |(\hat{\mathbf{g}}_{ml}^u)^H \mathbf{H}_{mi} (\hat{\mathbf{g}}_{ik}^d)^*|^2 \} &= \gamma_{ml}^u \mathbb{E}\{ (\hat{\mathbf{g}}_{ik}^d)^T \mathbb{E}\{ \mathbf{H}_{mi}^H \mathbf{H}_{mi} \} (\hat{\mathbf{g}}_{ik}^d)^* \} \\ &= N_r \gamma_{ml}^u \beta_{\text{RI},mi} \gamma_{\text{RI}} \mathbb{E}\{ (\hat{\mathbf{g}}_{ik}^d)^T (\hat{\mathbf{g}}_{ik}^d)^* \} = N_r N_t \gamma_{ml}^u \gamma_{ik}^d \beta_{\text{RI},mi} \gamma_{\text{RI}}. \end{aligned} \quad (\text{A5})$$

We next obtain the noise power for the l th uplink UE as

$$\mathbb{E}\{ |\mathbf{N}_l^u|^2 \} = \tilde{a}^2 \sum_{m \in \mathcal{M}_l^u} \mathbb{E}\{ |(\hat{\mathbf{g}}_{ml}^u)^H \mathbf{w}_m^u|^2 \} \stackrel{(a)}{=} \tilde{a}^2 N_r \sum_{m \in \mathcal{M}_l^u} \gamma_{ml}^u. \quad (\text{A6})$$

Equality (a) is because: i) estimated channel $\hat{\mathbf{g}}_{ml}^u$ and receiver noise \mathbf{w}_m^u are uncorrelated, and

$$\text{ii) } \mathbb{E}\{ |(\hat{\mathbf{g}}_{ml}^u)^H \mathbf{w}_m^u|^2 \} = \mathbb{E}\{ (\mathbf{w}_m^u)^H \mathbb{E}\{ \hat{\mathbf{g}}_{ml}^u (\hat{\mathbf{g}}_{ml}^u)^H \} \mathbf{w}_m^u \} = \gamma_{ml}^u \mathbb{E}\{ (\mathbf{w}_m^u)^H \mathbf{w}_m^u \} = N_r \gamma_{ml}^u. \quad (\text{A7})$$

Total quantization distortion for the l th uplink UE is given as

$$\begin{aligned} \mathbb{E}\{ |\text{TQD}_l^u|^2 \} &\approx (\tilde{b} - \tilde{a}^2) \sum_{m \in \mathcal{M}_l^u} \mathbb{E}\{ |(\hat{\mathbf{g}}_{ml}^u)^H \mathbf{y}_m|^2 \}, \text{ where} \\ \mathbb{E}\{ |(\hat{\mathbf{g}}_{ml}^u)^H \mathbf{y}_m|^2 \} &= N_r^2 \rho_u (\gamma_{ml}^u)^2 \theta_l + \rho_u N_r \gamma_{ml}^u \sum_{q=1}^{K_u} \beta_{mq}^u \theta_q \\ &\quad + \tilde{b} N_r N_t \rho_d \sum_{i=1}^M \sum_{k \in \kappa_{di}} \gamma_{ml}^u \gamma_{ik}^d \beta_{\text{RI},mi} \gamma_{\text{RI}} \eta_{ik} + N_r \gamma_{ml}^u. \end{aligned} \quad (\text{A8})$$

To obtain this result, we first note that the term TQD_l^u is the sum of the quantization distortions on all the fronthaul links due to the l th uplink UE, i.e., $\text{TQD}_l^u = \sum_{m \in \mathcal{M}_l^u} \zeta_{ml}^u$, as expressed in Eq. (12) of the manuscript. We assume that the quantization distortion is uncorrelated across the fronthaul links, which is shown to be a reasonably tight approximation to the exact behaviour for cell-free massive MIMO [12]. We note that the undistorted uplink signal for the l th uplink UE at the fronthaul of the m th AP is given as $(\hat{\mathbf{g}}_{ml}^u)^H \mathbf{y}_m$, as expressed in Eq. (6). Using these facts and by employing the optimal uniform quantization model as proposed in Appendix A, we express the TQD power for the l th uplink UE as follows

$$\mathbb{E}\{ |\text{TQD}_l^u|^2 \} \approx \sum_{m \in \mathcal{M}_l^u} \mathbb{E}\{ |\zeta_{ml}^u|^2 \} \approx (\tilde{b} - \tilde{a}^2) \sum_{m \in \mathcal{M}_l^u} \mathbb{E}\{ |(\hat{\mathbf{g}}_{ml}^u)^H \mathbf{y}_m|^2 \}.$$

We now need to calculate the power of the undistorted received signal after MRC at the m th AP for the l th uplink UE, i.e., $\mathbb{E}\{ |(\hat{\mathbf{g}}_{ml}^u)^H \mathbf{y}_m|^2 \}$. We first rewrite the expression for the undistorted,

MR combined uplink signal at the m th AP as follows

$$\begin{aligned}
(\hat{\mathbf{g}}_{ml}^u)^H \mathbf{y}_m^u &= \sum_{q=1}^{K_u} (\hat{\mathbf{g}}_{ml}^u)^H \mathbf{g}_{mq}^u x_q^u + \sum_{i=1}^M (\hat{\mathbf{g}}_{ml}^u)^H \mathbf{H}_{mi} \mathbf{x}_i^d + (\hat{\mathbf{g}}_{ml}^u)^H \mathbf{w}_m^u \\
&= \underbrace{\sqrt{\rho_u} (\hat{\mathbf{g}}_{ml}^u)^H \mathbf{g}_{ml}^u \sqrt{\theta_l} s_l^u}_{\text{message signal}} + \underbrace{\sqrt{\rho_u} \sum_{q=1, q \neq l}^{K_u} (\hat{\mathbf{g}}_{ml}^u)^H \mathbf{g}_{mq}^u \sqrt{\theta_q} s_q^u}_{\text{multi-user interference, MUI}_l^u} \\
&\quad + \underbrace{\sqrt{\rho_d} \sum_{i=1}^M \sum_{k \in \kappa_{di}} (\hat{\mathbf{g}}_{ml}^u)^H \mathbf{H}_{mi} (\hat{\mathbf{g}}_{ik}^d)^* (\tilde{a} \sqrt{\eta_{ik}} s_k^d + \varsigma_{ik}^d)}_{\text{intra-/inter-AP residual interference, RI}_l^u} + \underbrace{(\hat{\mathbf{g}}_{ml}^u)^H \mathbf{w}_m^u}_{\text{additive noise at APs, N}_l^u}.
\end{aligned}$$

Complication due to FD architecture: We note that for the FD CF mMIMO system, the presence of these *intra-/inter-AP RI terms* in the uplink signal complicates the analysis significantly. The precoded signal for the k th downlink UE is received at the i th AP after *quantization* in the fronthaul, which further complicates the analysis. This implies that the undistorted signal from the CPU, $\sqrt{\eta_{ik}} s_k^d$ is received in the distorted form $\mathcal{Q}\{\sqrt{\eta_{ik}} s_k^d\} = \tilde{a} \sqrt{\eta_{ik}} s_k^d + \varsigma_{ik}^d$, with $\mathbb{E}\{|\varsigma_{ik}^d|^2\} = (\tilde{b} - \tilde{a}^2) \eta_{ik}$, as shown in Eq. (1) of the manuscript. Finally, this combined undistorted signal goes through further *quantization* before reaching the CPU, which causes distortion yet again. To the best of our knowledge, no previous work investigates this coupling of the FD intra-/inter-AP RI terms with distortions introduced by the quantization procedure for limited fronthaul capacity.

To accurately model the RI term in the limited fronthaul capacity setting and compute the corresponding power, we propose the following lemma.

Lemma 1. The intra-/inter-AP RI contribution to the TQD power for the l th uplink UE in a FD CF mMIMO system with MRT/MRC transceiver is expressed as

$$\mathbb{E}\{|\text{TQD}_l^u|^2\}_{\text{RI}} \approx (\tilde{b} - \tilde{a}^2) \tilde{b} N_r N_t \rho_d \sum_{m \in \mathcal{M}_l^u} \sum_{i=1}^M \sum_{k \in \kappa_{di}} \gamma_{ml}^u \gamma_{ik}^d \beta_{\text{RI}, mi} \gamma_{\text{RI} ik} N_r \gamma_{ml}^u.$$

Proof: We express the intra-/inter-AP RI power of the undistorted, MR combined received

signal for the l th uplink UE as

$$\begin{aligned}
\mathbb{E}\{|\mathbf{RI}_l^u|^2\} &= \rho_d \sum_{i=1}^M \sum_{k \in \kappa_{di}} \mathbb{E}\{ |(\hat{\mathbf{g}}_{ml}^u)^H \mathbf{H}_{mi} (\hat{\mathbf{g}}_{ik}^d)^* (\tilde{a} \sqrt{\eta_{ik}} s_k^d + \zeta_{ik}^d) |^2 \} \\
&\stackrel{(a)}{=} \rho_d \sum_{i=1}^M \sum_{k \in \kappa_{di}} \mathbb{E}\{ |(\hat{\mathbf{g}}_{ml}^u)^H \mathbf{H}_{mi} (\hat{\mathbf{g}}_{ik}^d)^* (\tilde{a} \sqrt{\eta_{ik}} s_k^d + \zeta_{ik}^d) |^2 \tilde{b} \eta_{ik} \} \\
&\stackrel{(b)}{=} \tilde{b} N_r N_t \rho_d \sum_{i=1}^M \sum_{k \in \kappa_{di}} \gamma_{ml}^u \gamma_{ik}^d \beta_{\text{RI},mi} \gamma_{\text{RI}} \eta_{ik} N_r \gamma_{ml}^u.
\end{aligned}$$

Equality (a) follows from these facts: i) downlink distorted signal $\tilde{a} \sqrt{\eta_{ik}} s_k^d$ and the quantization noise ζ_{ik}^d , are uncorrelated, and ii) $\mathbb{E}\{|\zeta_{ik}^d|^2\} = (\tilde{b} - \tilde{a}^2) \eta_{ik}$. Equality (b) is because: i) channels $\hat{\mathbf{g}}_{ml}^u$, \mathbf{H}_{mi} and $\hat{\mathbf{g}}_{mk}^d$ are mutually independent; ii) $\gamma_{\text{RI},mi} = \beta_{\text{RI},mi} \gamma_{\text{RI}}$, $i = 1$ to M ; and iii) the result

$$\begin{aligned}
\mathbb{E}\{ |(\hat{\mathbf{g}}_{ml}^u)^H \mathbf{H}_{mi} (\hat{\mathbf{g}}_{ik}^d)^* |^2 \} &= \mathbb{E}\{ (\hat{\mathbf{g}}_{ik}^d)^T \mathbb{E}\{ \mathbf{H}_{mi}^H \mathbb{E}\{ (\hat{\mathbf{g}}_{ml}^u) (\hat{\mathbf{g}}_{ml}^u)^H \} \mathbf{H}_{mi} \} (\hat{\mathbf{g}}_{ik}^d)^* \} \\
&= \gamma_{ml}^u \mathbb{E}\{ (\hat{\mathbf{g}}_{ik}^d)^T \mathbb{E}\{ \mathbf{H}_{mi}^H \mathbf{H}_{mi} \} (\hat{\mathbf{g}}_{ik}^d)^* \} \\
&= N_r \gamma_{ml}^u \beta_{\text{RI},mi} \gamma_{\text{RI}} \mathbb{E}\{ (\hat{\mathbf{g}}_{ik}^d)^T (\hat{\mathbf{g}}_{ik}^d)^* \} = N_r N_t \gamma_{ml}^u \gamma_{ik}^d \beta_{\text{RI},mi} \gamma_{\text{RI}}.
\end{aligned}$$

Using the above expression for $\mathbb{E}\{|\mathbf{RI}_l^u|^2\}$, we obtain the intra-/inter-AP RI contribution to the TQD power as follows

$$\begin{aligned}
\mathbb{E}\{|\text{TQD}_l^u|^2\}_{\text{RI}} &\approx (\tilde{b} - \tilde{a}^2) \sum_{m \in \mathcal{M}_l^u} \mathbb{E}\{|\mathbf{RI}_l^u|^2\} \\
&= (\tilde{b} - \tilde{a}^2) \tilde{b} N_r N_t \rho_d \sum_{m \in \mathcal{M}_l^u} \sum_{i=1}^M \sum_{k \in \kappa_{di}} \gamma_{ml}^u \gamma_{ik}^d \beta_{\text{RI},mi} \gamma_{\text{RI}} \eta_{ik} N_r \gamma_{ml}^u.
\end{aligned}$$

■

The result in (15) follows from the following expression

$$S_l^u = \tau_f \log_2 \left(1 + \frac{\mathbb{E}\{|\text{DS}_l^u|^2\}}{\mathbb{E}\{|\text{BU}_l^u|^2\} + \mathbb{E}\{|\text{MUI}_l^u|^2\} + \mathbb{E}\{|\mathbf{RI}_l^u|^2\} + \mathbb{E}\{|\text{TQD}_l^u|^2\} + \mathbb{E}\{|\mathbf{N}_l^u|^2\}} \right).$$

We now derive the achievable SE expression for the k th downlink UE in (14). From Section II, we know that $\mathbf{g}_{mk}^d = \hat{\mathbf{g}}_{mk}^d + \mathbf{e}_{mk}^d$, where $\hat{\mathbf{g}}_{mk}^d$ and \mathbf{e}_{mk}^d are independent and $\mathbb{E}\{\|\hat{\mathbf{g}}_{mk}^d\|^2\} = N_t \gamma_{mk}^d$.

We can express the desired signal for the k th downlink UE as

$$\mathbb{E}\{|\text{DS}_k^d|^2\} = \tilde{a}^2 \rho_d \mathbb{E} \left\{ \left| \sum_{m \in \mathcal{M}_k^d} \sqrt{\eta_{mk}} \mathbb{E}\{ (\hat{\mathbf{g}}_{mk}^d)^T (\hat{\mathbf{g}}_{mk}^d)^* \} s_k^d \right|^2 \right\} = \tilde{a}^2 N_t^2 \rho_d \left(\sum_{m \in \mathcal{M}_k^d} \sqrt{\eta_{mk}} \gamma_{mk}^d \right)^2. \quad (\text{A9})$$

We now calculate the beamforming uncertainty for the k th downlink UE as

$$\begin{aligned}\mathbb{E}\{|\text{BU}_k^d|^2\} &= \tilde{a}^2 \rho_d \sum_{m \in \mathcal{M}_k^d} \mathbb{E}\{|\sqrt{\eta_{mk}} ((\mathbf{g}_{mk}^d)^T (\hat{\mathbf{g}}_{mk}^d)^* - \mathbb{E}\{(\mathbf{g}_{mk}^d)^T (\hat{\mathbf{g}}_{mk}^d)^*\})|^2\} \\ &\stackrel{(a)}{=} \tilde{a}^2 \rho_d \sum_{m \in \mathcal{M}_k^d} \eta_{mk} (N_t(N_t+1)(\gamma_{mk}^d)^2 + N_t \gamma_{mk}^d (\beta_{mk}^d - \gamma_{mk}^d) - N_t^2 (\gamma_{mk}^d)^2) = \tilde{a}^2 N_t \rho_d \sum_{m \in \mathcal{M}_k^d} \eta_{mk} \beta_{mk}^d \gamma_{mk}^d.\end{aligned}\quad (\text{A10})$$

Equality (a) is obtained by i) using $\mathbb{E}\{|s_k^d|^2\} = 1$; ii) substituting $\mathbf{g}_{mk}^d = \hat{\mathbf{g}}_{mk}^d + \mathbf{e}_{mk}^d$; iii) using the fact that $\hat{\mathbf{g}}_{mk}^d$ are zero-mean and uncorrelated; and iv) using the results $\mathbb{E}\{\|\hat{\mathbf{g}}_{mk}^d\|^4\} = N_t(N_t+1)(\gamma_{mk}^d)^2$ [5] and $\mathbb{E}\{\|\mathbf{e}_{mk}^d\|^2\} = (\beta_{mk}^d - \gamma_{mk}^d)$.

We now simplify the multi-UE interference for the k th downlink UE as

$$\mathbb{E}\{|\text{MUI}_k^d|^2\} = \tilde{a}^2 \rho_d \sum_{m=1}^M \sum_{q \in \kappa_{dm} \setminus k} \eta_{mq} \mathbb{E}\{|\mathbf{g}_{mk}^d{}^T (\hat{\mathbf{g}}_{mq}^d)^*|^2\} \stackrel{(a)}{=} \tilde{a}^2 N_t \rho_d \sum_{m=1}^M \sum_{q \in \kappa_{dm} \setminus k} \beta_{mk}^d \eta_{mq} \gamma_{mq}^d. \quad (\text{A11})$$

Equality (a) is because: i) $\mathbb{E}\{|s_q^d|^2\} = 1$; ii) $\hat{\mathbf{g}}_{mq}^d$ and \mathbf{g}_{mk}^d are mutually independent; and

$$\text{iii) } \mathbb{E}\{|\mathbf{g}_{mk}^d{}^T (\hat{\mathbf{g}}_{mq}^d)^*|^2\} = \mathbb{E}\{(\hat{\mathbf{g}}_{mq}^d)^T \mathbb{E}\{(\mathbf{g}_{mk}^d)^* (\mathbf{g}_{mk}^d)^T\} (\hat{\mathbf{g}}_{mq}^d)^*\} = N_t \beta_{mk}^d \gamma_{mq}^d.$$

We now calculate the uplink downlink interference for the k th downlink UE as follows

$$\mathbb{E}\{|\text{UDI}_k^d|^2\} = \rho_u \sum_{l=1}^{K_u} \mathbb{E}\{|h_{kl}|^2\} \theta_l \stackrel{(a)}{=} \rho_u \sum_{l=1}^{K_u} \tilde{\beta}_{kl} \theta_l. \quad (\text{A12})$$

Equality (a) follows from i) $\mathbb{E}\{|h_{kl}|^2\} = \tilde{\beta}_{kl} \mathbb{E}\{|\tilde{h}_{kl}|^2\} = \tilde{\beta}_{kl}$; ii) $\mathbb{E}\{|s_l^u|^2\} = 1$. We express the total quantization distortion for the k th downlink UE as

$$\mathbb{E}\{|\text{TQD}_k^d|^2\} \approx \rho_d \sum_{m=1}^M \sum_{q \in \kappa_{dm}} \mathbb{E}\{|\mathbf{g}_{mk}^d{}^T (\hat{\mathbf{g}}_{mq}^d)^* \varsigma_{mq}^d|^2\} \stackrel{(a)}{=} (\tilde{b} - \tilde{a}^2) N_t \rho_d \sum_{m=1}^M \sum_{q \in \kappa_{dm}} \beta_{mk}^d \eta_{mq} \gamma_{mq}^d. \quad (\text{A13})$$

Equality (a) is because: i) $\mathbb{E}\{|\varsigma_{mk}^d|^2\} = (\tilde{b} - \tilde{a}^2) \eta_{mk}$; ii) quantization distortion ς_{mq}^d is independent of the wireless channels \mathbf{g}_{mk}^d and $\hat{\mathbf{g}}_{mq}^d$; and iii) of the following result:

$$\begin{aligned}\mathbb{E}\{|\mathbf{g}_{mk}^d{}^T (\hat{\mathbf{g}}_{mq}^d)^* \varsigma_{mq}^d|^2\} &= \mathbb{E}\{|\mathbf{g}_{mk}^d{}^T (\hat{\mathbf{g}}_{mq}^d)^*|^2\} \mathbb{E}\{|\varsigma_{mq}^d|^2\} = (\tilde{b} - \tilde{a}^2) \eta_{mq} \mathbb{E}_{\hat{\mathbf{g}}_{mq}^d} \{(\hat{\mathbf{g}}_{mq}^d)^T \beta_{mk}^d \mathbf{I}_{N_t} (\hat{\mathbf{g}}_{mq}^d)^*\} \\ &= (\tilde{b} - \tilde{a}^2) \eta_{mq} \beta_{mk}^d \mathbb{E}_{\hat{\mathbf{g}}_{mq}^d} \{(\hat{\mathbf{g}}_{mq}^d)^T (\hat{\mathbf{g}}_{mq}^d)^*\} = (\tilde{b} - \tilde{a}^2) N_t \beta_{mk}^d \eta_{mq} \gamma_{mq}^d.\end{aligned}$$

Result in (14) follows from the following expression for the achievable SE lower bound:

$$S_k^d = \tau_f \log_2 \left(1 + \frac{\mathbb{E}\{|\text{DS}_k^d|^2\}}{\mathbb{E}\{|\text{BU}_k^d|^2\} + \mathbb{E}\{|\text{MUI}_k^d|^2\} + \mathbb{E}\{|\text{UDI}_k^d|^2\} + \mathbb{E}\{|\text{TQD}_k^d|^2\} + \mathbb{E}\{|w_k^d|^2\}} \right).$$